ACS Energy LETTERS

http://pubs.acs.org/journal/aelccp

FOCUS REVIEW

Y-Series-Based Polymer Acceptors for High-Performance All-Polymer Solar Cells in Binary and Non-binary Systems

Meenal Kataria,[‡] Hong Diem Chau,[‡] Na Yeon Kwon, Su Hong Park, Min Ju Cho,* and Dong Hoon Choi*

Cite This: *ACS Energy Lett.* 2022, 7, 3835−3854

Read Online

ACCESS | Metrics & More | Article Recommendations

ABSTRACT: **Recently, all-polymer solar cells (all-PSCs) have made significant progress in terms of efficiency and performance. Using Y-series-based small-molecule acceptors, a new range of polymer acceptors for all-PSC has been developed. These synthesized polymer acceptors have a low band gap, broad absorption, and easily tunable energy levels, making them suitable n-type candidates for efficient all-PSCs. In this review, we summarize some molecular design and synthesis strategies used to advance the field of innovative materials and device engineering involving Y-series-based polymer acceptors to achieve a power conversion efficiency greater than 18% in all-PSCs.**

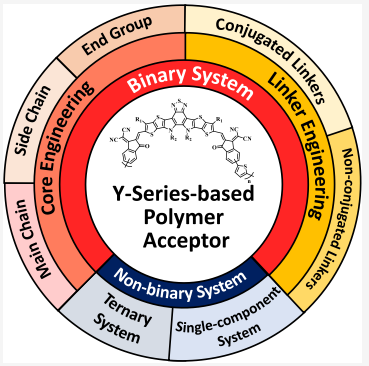

Recent research has shown that bulk heterojunction (BHJ) all-polymer solar cells (PSCs) comprising conjugated polymer donor and acceptor blends can produce large-area devices[1−4] at low cost and with a simple solution process;[5−8] moreover, they possess outstanding thermal and mechanical stabilities.[9−13] Until the development of a new type of polymer acceptor by Zhang et al. in 2017,[14] the power conversion efficiency (PCE) of all-PSCs using donor−acceptor (D-A)-type polymers did not surpass 12% due to their low extinction coefficient and narrow absorption spectrum (300−700 nm).[15−17] Zhang et al. proposed a strategy to polymerize A-D-A-type small-molecule acceptors (SMAs) with a low band gap to develop a novel polymer acceptor, PZ1, containing an IDIC accepting unit and a thiophene linker; a PCE value of 13% has been attained with the continued development of IDIC- or ITIC-based polymer acceptors.[14,18−22] It has been observed that these polymer acceptors retain all the benefits associated with A-D-A-type SMAs as well as the distinctive properties of the polymer backbone.

In addition, many researchers recognized the advantages of Y-series-type SMA with superior device performance and predicted that establishing Y-series-based polymer acceptors in all-PSCs would be a significant step forward in the future of PSCs. Since the first A-DA′D-A-type pentacyclic SMA, named BZIC, was announced in 2017,[23] a series of high-performance Y-series-based SMAs have been developed by introducing a heptacyclic fused ring into the conventional structure,[24] using halogenated end groups,[25,26] and replacing the benzotriazole (BTA) core with a benzothiadiazole (BT) core.[27] In contrast to A-D-A-type SMAs,[28−31] Y-series-type SMAs exhibit a distinct A-DA′D-A core structure and have proven to be the most promising candidate to date, primarily attributable to their outstanding characteristics, such as (i) an extended absorption range to 950 nm, (ii) molecular packing to form a 3D interpenetrating network for efficient charge transport and exciton delocalization, and (iii) electron mobility in the range 10^{-4} to 10^{-3} cm^2 V^{-1} s^{-1} with exceptionally low energy loss. The corresponding Y-series-based polymer acceptors also overcome the limitations of D-A-type and A-D-A-type polymer acceptors by reducing the energy loss for high short-circuit current density (J_{sc}) and open-circuit voltage (V_{oc}) and by suppressing unfavorable charge-transfer states and charge carrier recombination.[32−34] Since the first Y-series-based

Received: July 5, 2022
Accepted: September 29, 2022

https://doi.org/10.1021/acsenergylett.2c01541
ACS Energy Lett. 2022, 7, 3835−3854

polymer acceptor was reported by Huang et al. in 2020,[33] this type of acceptors was deemed the best n-type materials. Very recently, all-PSCs containing Y-series-based polymer acceptor achieved a high PCE of 18%,[35] comparable to that of Y-series SMA-based devices.[36,37] Nevertheless, if flexible organic solar cells (OSCs) are to be considered in the future, the continuous development of a new polymer acceptor with superior thermal and mechanical stability is necessary. For such research, it is of the utmost importance to examine exhaustively all approaches utilized in the past three years with all-PSCs comprising polymer acceptors based on the Y-series SMAs.

Y-series-type small-molecule acceptors with outstanding characteristics exhibit a distinct A-DA′D-A core structure and can be introduced into polymer structures, proving to be the most promising candidate to date.

Several articles have recently discussed an all-PSCs development roadmap. Independently, Kim et al.[38] and Marks et al.[39] analyzed design strategies for polymer donors/acceptors and device efficiency enhancements for all-PSCs through 2019. Andersson et al. investigated the growth of n-type polymers for all-PSC devices through 2019.[40] Recently, Zhang and Li described a polymerized small-molecule acceptor strategy that utilizes IDIC, ITIC, and Y-series-based SMAs to generate novel polymer acceptors.[41] Kyaw et al. demonstrated the development of non-fullerene-based organic solar cells.[42] Despite all these review articles, it is necessary to summarize research data solely focused on the evolution of Y-series-based polymer acceptors and the various techniques for device fabrication employed to improve their stability and efficiency over the past three years.

In this review, polymer acceptors used in binary active layer systems are first introduced based on a variety of core structure and linker structure modifications. In addition, the materials comprising ternary and single-component active layers as a non-binary active layer system are described. This is followed by a conclusion and an outlook on the future of these acceptors. Figures 1−5 contain diagrammatic representations of all the polymers reviewed. The performance of photovoltaics is summarized in Tables 1 and 2.

The synthetic strategy involved in the development of Y-series-based polymer acceptors is the Stille cross-coupling between Y-series-based dibromide and the distannyl linking unit. From this design strategy, we can envisage that straightforward approaches to manipulating electronic properties and controlling intermolecular stacking and charge transport properties of these generated polymer acceptors involve deploying the properties of either Y-series-based SMA or the linking unit. Figure 1 illustrates the strategies that have been used to develop a diverse array of SMA building blocks involving the insertion of the alkyl chain, chemical modifications in the DA′D central core, the end group, and the position of the bromine at the end group of SMA.

As depicted in Figure 1, various conjugated and non-conjugated linkers, ranging from simple to bulky, electron-donating to electron-withdrawing units, have been utilized thus far. In addition to molecular design, controlling the molecular weight plays a crucial role in balancing the solubility of the material, the morphology of the blend film, and the stability of the device. Other strategies, including the insertion of a third unit into polymer chains (random terpolymers), introduction of third components with complementary properties (ternary

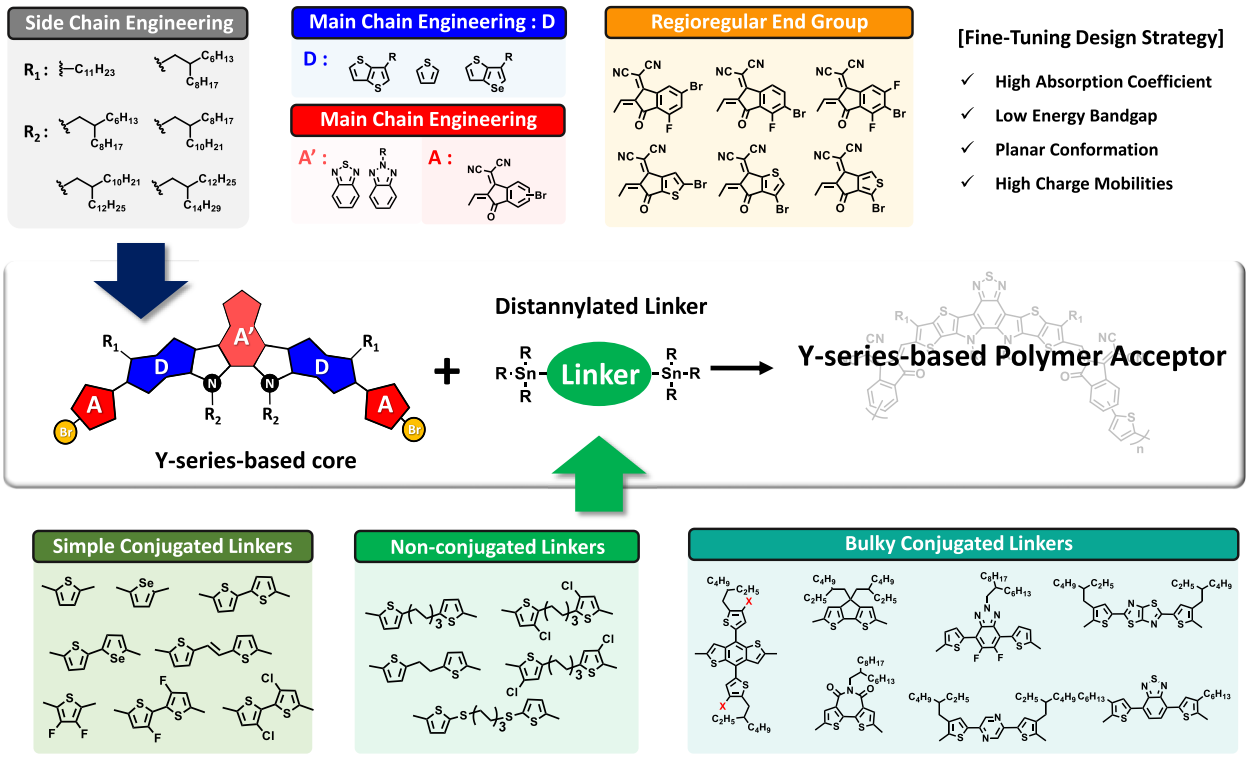

Figure 1. Schematic representation of the contents of the present Focus Review.

https://doi.org/10.1021/acsenergylett.2c01541
ACS Energy Lett. 2022, 7, 3835−3854

systems), and combinations of the donor polymer and these acceptors in a single component, have also been used.

1. POLYMER ACCEPTORS FOR THE BINARY ACTIVE LAYER

1.1. Core Design Strategies. For maximizing the device performance of all-PSCs, the polymer acceptors must have brilliant solubility, strong absorption coefficient (>10^5 cm^{-1}), ultra-narrow band gaps (1.6−1.3 eV) for broad absorption spectra (>900 nm), planar backbones, and better miscibility with polymer donors for favorable morphology to ensure a high J_{sc} (~29 mA cm^{-2}) and small energy loss (<0.5 eV) for the resulting devices. Additionally, the acceptors must possess high chemical, high thermal, high mechanical, and high photostabilities to create durable all-PSC devices. To attain these properties in binary all-PSCs, various design strategies for the SMA analog and linking units have been implemented.

For maximizing the device performance of all-polymer solar cells, the polymer acceptors must have brilliant solubility, strong absorption coefficient, ultra-narrow band gaps for broad absorption spectra, planar backbones, and better miscibility with polymer donors.

1.1.1. Side-Chain Engineering. The variation of the alkyl chain on the Y-series-based monomer from linear to branched and shorter to longer enhanced the solubility. Additionally, these alkyl chains on both the sides of the SMA assist with conformational issues and locking to achieve a reduced level of energetic disorder. Min et al. reported the synthesis of the polymer acceptor PYT1 from the monomer Y5-C20 having two 2-octyldodecyl as the *N*-alkyl side chains and thiophene as the conjugative linking unit (Figure 2).[32] The performance of PM6:PYT1 blend-based all-PSCs revealed a PCE of 13.43% (Table 1), which is substantially higher than that of the PM6:Y5-C20-based device owing to its superior crystalline domain formation and low donor−acceptor highest occupied molecular orbital (HOMO) energy offset. On the other hand, the effect of controlling the M_n value on the crystallinity, miscibility, and performance of all-PSC devices in the above polymer acceptor was investigated.[43] Consequently, a series of PYT polymer acceptors, i.e., PYT_L (M_n = 7.2 kDa), PYT_M (M_n = 12.3 kDa), and PYT_H (M_n = 20.6 kDa), with different M_n values were developed (Figure 2). Among them, the device performance of PM6:PYT_M is superior to that of other devices with a PCE value of 13.44% (Table 1) due to the improved miscibility, external quantum efficiency values, and low energy loss. These results indicated the role of M_n in device performance and found PYT-based binary devices with a medium M_n value demonstrated the best performance. For Y-based polymer acceptors, intermediate M_n polymers are preferred over those with low or high M_n values in most cases.[44−46] However, it should be recognized that the optimal molecular weight, which determines device performance, may vary depending on the chemical structure of the repeating group of the polymer acceptor. In contrast to the PYT series, Huang et al. discovered that polymer acceptors, PJ1 series, which have a slightly longer *N*-alkyl side chain in the core, are promising candidates for binary all-PSCs (Figure 2).[33] In comparison to PJ1-L (M_n = 7.3 kDa) and PJ1-M (M_n = 11.0 kDa)-based devices, the PCE of a PBDB-T:PJ1-H (M_n = 23.3 kDa)-based device was relatively high at 14.4% (Table 1). An increase in J_{sc} was observed in the device based on PBDB-T:PJ1-H as a result of red-shifted absorption and a slight increase in extinction coefficient. These findings suggest that the addition of a long alkyl chain to the PJ1 series can improve the solubility of higher M_n polymers, thereby improving the performance of the corresponding organic photovoltaic (OPV) devices. Therefore, since the molecular weight can directly affect the solubility, chain entanglement, chain packing behavior, and viscoelasticity of the polymer acceptor, it is important to optimize this M_n value for each polymer design to maximize the resulting device performance.

Sun et al. also synthesized a series of polymer acceptors PY-X (PY-HD, PY-OD, PY-DT, and PY-DH) by introducing various *N*-alkyl side chains and the branched 2-hexyldecyl chains at the *β*-position of the thiophene on the Y-series-based core (Figure 2).[47] Among them, the PM6:PY-DT-based binary device represented a breakthrough for all-PSCs with a PCE value of 16.76% with an increased V_{oc} of 0.949 V (Table 1). The increase in device performance can be attributed to (i) the up-shifting of the lowest unoccupied energy level (LUMO) and (ii) the increase in miscibility due to the lengthening of the branched *N*-alkyl chain. However, PM6:PY-DH demonstrated an inferior device performance due to disruptions in the molecular arrangement (or aggregation) in the solid-state as the length of the alkyl chain increased. Therefore, the alkyl chain should be selected with caution.

1.1.2. Main-Chain Engineering. The key strategy to finely tune the photovoltaic properties of the Y-series-based polymer acceptors lies in the modifications of the main chain. While the majority of reported Y-series-based polymer acceptors employed BT as the A′-core, the utilization of BTA core could give more advantages to adjust the solubility and molecular packing of the polymer chain through the additional alkyl side chain tethered to the nitrogen. For example, Li et al. introduced the polymer acceptor PN-Se with BTA core in comparison with the BT-based analog PS-Se (Figure 2).[48] Compared to PS-Se with stronger electron withdrawing BT core, PN-Se exhibited upshifted LUMO level. Besides, the extra alkyl chain on the BTA core had a positive effect on the packing behavior of PN-Se, proven by its more red-shifted absorption spectra as well as the formation of homogeneous fibril-like phases in the blend film with PBDB-T. As a result, the all-PSC based on PBDB-T:PN-Se showed an improved PCE of 16.16%, with significant enhancement in all parameters V_{oc}, J_{sc}, and FF compared to the PBDB-T:PS-Se-based device (Table 1). Jen et al. observed similar results with the polymers acceptors PYT, PZT, and PZT-*γ* (Figure 2).[49] Bearing the BTA core, PZT also revealed a bathochromic-shifted absorption spectra and shallower energy level than those of PYT with BT core. The regioregular isomer of PZT, PZT-*γ*, exhibited further broadened absorption spectra, as well as improved blend morphology with donor polymer. As a result, the binary device of PBDB-T:PZT-*γ* outperformed with PCE of 15.8% (Table 1) with a significantly higher J_{sc} of 24.7 mA cm^{-2} and a low energy loss of 0.51 eV.

Zhou et al. demonstrated the polymer acceptors based on Y-series moiety bearing the BTA unit in DA′D fused central core by keeping in mind that the alkyl chain will help in providing

https://doi.org/10.1021/acsenergylett.2c01541
ACS Energy Lett. 2022, 7, 3835−3854

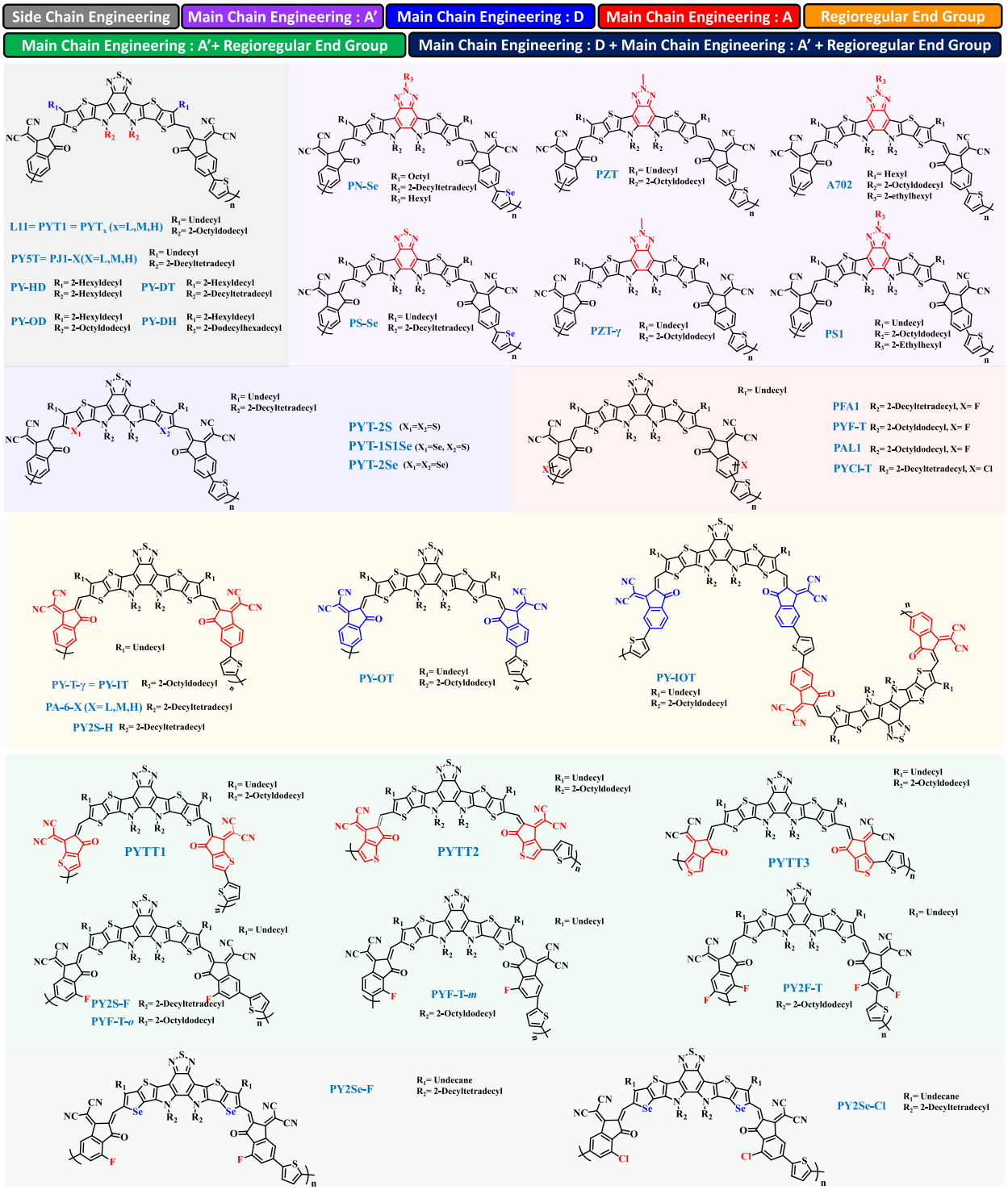

Figure 2. Design strategies for Y-series-based core and corresponding structures of various polymer acceptors.

good solubility (Figure 2).[50] The all-PSCs bearing A702 and PBDB-T generate PCE of 11.84% along with a high V_{oc} of 0.90 V (Table 1). In contrast, all-PSCs containing a binary mixture of A702 and PM6 under similar optimized conditions showed only a 2.66% PCE value which is due to the deep HOMO level of PM6 with respect to polymer acceptor. Consequently, it interfered with proper charge transfer, resulting in lower J_{sc} and FF. In parallel to the work on A702 polymer acceptor, Ying et al.[51] employed the longer alkyl chain on the central fused BTA core and synthesized the polymer acceptor named as PS1. Intriguingly, the devices were fabricated using 2-methyltetrahydrofuran (2-MeTHF) as a non-chlorinated and green processing solvent system. The J_{sc} and V_{oc} values were improved from 0.90 V to 0.92 V and 21.93 mA cm^{-2} to 22.47 mA cm^{-2}, respectively, along with an advancement in PCE value from 11.84% to 13.8% (Table 1). From these results, it was found that increasing the length of the alkyl chain improved the solubility in 2-MeTHF and improved the crystallinity of the polymer, and consequently the tendency to increase J_{sc} and FF.

https://doi.org/10.1021/acsenergylett.2c01541
ACS Energy Lett. 2022, 7, 3835−3854

Table 1. Photovoltaic Parameters of the All-PSCs Binary Systems

SMA	polymer acceptor	polymer donor	PA HOMO/LUMO (eV)	λ_{peak} (nm)[a] max/onset	μ_h/μ_e (10^{-4} cm^2 V^{-1} s^{-1})[b]	V_{oc} (V)	J_{sc} (mA cm^{-2})	FF (%)	PCE (%)	ref
Y5-C20	PYT1 and CN additive	PM6	−5.69/−3.92	801/875	1.08/3.62	0.938	21.50	66.66	13.43	32
Y5-C20-Br	PYT_L (7.2)	PM6	−5.73/−3.92	806/882	2.81/7.88	0.93	20.92	64.51	12.55	43
Y5-C20-Br	PYT_M (12.3)	PM6	−5.69/−3.92	799/875	6.12/8.91	0.93	21.78	66.33	13.44	43
Y5-C20-Br	PYT_H (20.6)	PM6	−5.69/−3.93	792/859	2.49/5.92	0.95	20.6	52.91	8.61	43
TTPBT-IC	PJ1-L (7.3)	PBDB-T	−5.68/−3.83	786/868	55.8/2.31	0.89	20.3	69	12.3	33
TTPBT-IC	PJ1-M (11.0)	PBDB-T	−5.67/−3.83	793/872	65.6/3.34	0.88	21.6	70	13.2	33
TTPBT-IC	PJ1-H (23.3)	PBDB-T	−5.64/−3.82	798/880	24.7/7.09	0.90	22.3	70	14.1	33
SMA-OD	PY-OD	PM6	−5.60/−3.84	788/832	5.58/4.20	0.943	23.95	73.2	16.53	47
SMA-DT	PY-DT	PM6	−5.60/−3.83	788/832	4.32/3.53	0.949	23.73	74.4	16.76	47
SMA-DH	PY-DH	PM6	−5.65/−3.76	766/832	3.95/1.74	0.961	21.39	72.3	14.86	47
SMA-HD	PY-HD	PM6	−5.52/−3.94	788/837	7.11/5.37	0.937	24.05	72.8	16.41	47
TPBN-Br	PN-Se	PBDB-T	−5.63/−3.85	820/905	7.92/6.87	0.907	24.82	71.8	16.16	48
TPBS-Br	PS-Se	PBDB-T	−5.69/−3.88	798/879	6.89/4.84	0.874	23.27	68.0	13.83	48
–	PYT	PBDB-T	−5.64/−3.81	795/873	2.73/3.44	0.892	20.8	69.6	12.9	49
ZIC-Br	PZT	PBDB-T	−5.58/−3.76	817/895	2.47/3.31	0.909	23.2	68.6	14.5	49
ZIC-Br-γ	PZT-γ	PBDB-T	−5.57/−3.78	838/913	4.35/5.07	0.896	24.7	71.3	15.8	49
TPBTA-2Br	A702	PM6	−5.41/−3.75	815/892	5.34/1.08	0.95	6.74	43	2.73	50
TPBTA-2Br	A702	PBDB-T	−5.41/−3.75	815/892	2.10/1.02	0.90	21.93	60	11.84	50
TTPTAZ-ICBr	PS1	PTzBI-oF	−5.56/−3.70	810/892	2.45/3.57	0.92	22.47	66.70	13.8	51
–	PYT-2S	PM6	−5.56/−3.72	810/878	4.49/7.18	0.941	22.3	70.7	14.8	52
1S1Se-ICBr	PYT-1S1Se	PM6	−5.61/−3.75	824/890	4.99/8.50	0.926	24.1	73.0	16.3	52
2Se-ICBr	PYT-2Se	PM6	−5.59/−3.79	830/902	3.51/7.37	0.908	23.9	71.4	15.5	52
Y5-Br	PY5T	PTzBI-oF	−5.71/−3.76	792/852	3.76/0.833	0.91	9.91	44.42	4.01	53
Y5-F-Br	PFA1	PTzBI-oF	−5.74/−3.84	815/881	10.3/5.49	0.87	23.96	72.67	15.11	53
Y-OD-Br	PY-T	PM6	−5.63/−380	796/875	6.17/7.37	0.95	17.45	64.61	10.74	54
Y-OD-FBr	PYF-T	PM6	−5.67/−3.72	821/900	7.52/8.64	0.88	23.27	66.83	13.77	54
BTP-OD-FBr	PAL1	PM6	−5.67/−3.78	811/890	0.876/0.658	0.91	22.41	66.32	13.53	55
BTP-OD-HBr	PAL2	PM6	−5.60/−3.81	818/888	0.494/0.297	0.90	17.96	56.46	9.16	55
Y5-IT	PY-IT	PM6	−5.68/−3.94	808/894	9.21/5.28	0.933	22.30	72.3	15.05	56
Y5-OT	PY-OT	PM6	−5.69/−3.90	791/874	8.79/3.81	0.954	16.82	62.6	10.04	56
Y5-IOT	PY-IOT	PM6	−5.68/−3.92	796/882	9.03/4.57	0.939	19.71	65.6	12.12	56
M-6	PA-6-L (8.9)	JD-40	−5.67/−3.80	796/870	12.86/1.77	0.92	22.13	72.99	14.81	44
M-6	PA-6-M (12.5)	JD-40	−5.64/−3.78	792/872	15.03/2.13	0.92	22.42	72.41	14.99	44
M-6	PA-6-H (30.1)	JD-40	−5.65/−3.75	795/854	22.19/1.85	0.92	20.53	67.36	12.78	44
CPTCN-Br	PYTT-1	PBDB-T	−5.66/ −3.82	761/834	2.22/1.22	0.93	20.66	70.35	13.54	57, 58
CPTCN-Br1	PYTT-2	PBDB-T	−5.73/−3.83	769/832	1.19/0.584	0.91	22.00	71.53	14.32	57, 58
CPTCN-Br2	PYTT-3	PBDB-T	−5.76/−3.88	815/861	1.01/0.179	0.82	21.99	68.47	12.41	57, 58
Y-OD-FBr-*o*	PYF-T-*o*	PM6	−5.73/−3.81	800/896	8.4/7.8	0.901	23.3	72.4	15.2	45
Y-OD-FBr-*m*	PYF-T-*m*	PM6	−5.73/−3.77	758/880	1.21/2.7	0.949	4.60	32.7	1.40	45
Y-OD-2FBr	PY2F-T	PM6	−5.71/−3.84	830/904	8.20/9.29	0.86	24.02	72.62	15.22	59
Y2SBr-H	PY2S-H	PM6	−5.76/−3.87	810/852	4.49/7.18	0.941	22.3	70.7	14.8	60
Y2SBr-F	PY2S-F	PM6	−5.78/−3.91	818/867	4.66/7.62	0.920	23.3	70.5	15.1	60
Y2SeBr-F	PY2Se-F	PM6	−5.76/−3.93	839/876	4.54/9.34	0.885	24.4	72.2	15.6	60
Y2SeBr-Cl	PY2Se-Cl	PM6	−5.75/−3.93	837/875	5.11/9.64	0.884	24.5	74.3	16.1	60
Y5-C20	PY-O	PBDB-T	−5.57/ −3.78	793/855	1.56/2.04	0.876	17.86	62.68	9.80	61
Y5-C20	PY-S	PBDB-T	−5.55/ −3.78	801/864	2.55/2.74	0.889	22.84	69.71	14.16	61
Y5-C20	PY-Se	PBDB-T	−5.56/ −3.77	793/874	3.28/3.16	0.891	23.52	73.85	15.48	61
Y5-Br	PY-2T	PBDB-T	−5.59/−3.78	791/905	−/2.7	0.89	11.56	51	5.34	62
Y5-Br	PY-2T2Cl	PBDB-T	−5.63/−3.82	793/895	−/3.8	0.87	16.32	65	9.35	62
m-Br-BTIC	PBTIC-γ-2F2T	PM6	−5.51/−3.77	805/882	2.6/1.8	0.95	22.56	66.89	14.34	63
m-Br-BTIC	PBTIC-γ-2T	PM6	−5.56/−3.80	796/871	0.13/0.57	0.95	20.85	60.22	11.92	63
Y5-C20-Br- γ	PY-V-γ	PM6	−5.64/−3.76	796/881	3.15/4.80	0.912	24.8	75.8	17.1	64
Y5-C20-Br- γ	PY-T-γ	PM6	−5.63/−3.73	810/871	5.29/12	0.929	24.1	71.9	16.1	64
Y5-C20-Br-γ	PY-2T-γ	PM6	−5.62/−3.69	789/867	1.42/3.01	0.933	23.5	69.9	15.3	64
TTPBT-IC	PJTET	JD-40	−5.56/−3.78	776/835	11.4/8.55	0.92	18.58	63.84	10.93	65
TTPBT-IC	PJTVT	JD-40	−5.57/−3.77	787/869	3.14/1.19	0.89	23.57	76.40	16.13	65
TPBT-Br	PTPBT	PBDBT	−5.66/−3.85	800/873	4.71/2.59	0.849	19.82	59.2	9.96	66
TPBT-Br	PTPBTET0.1	PBDBT	−5.66/−3.85	800/873	4.91/2.48	0.855	19.48	62.3	10.37	66
TPBT-Br	PTPBTET0.2	PBDBT	−5.66/−3.84	800/879	5.82/2.91	0.864	20.78	65.5	11.76	66

https://doi.org/10.1021/acsenergylett.2c01541
ACS Energy Lett. 2022, 7, 3835−3854

Table 1. continued

SMA	polymer acceptor	polymer donor	PA HOMO/LUMO (eV)	λ_{peak} (nm)[a] max/onset	μ_h/μ_e (10^{-4} cm^2 V^{-1} s^{-1})[b]	V_{oc} (V)	J_{sc} (mA cm^{-2})	FF (%)	PCE (%)	ref
TPBT-Br	PTPBTET0.3	PBDBT	−5.65/−3.83	800/879	7.27/4.13	0.899	21.33	65.3	12.52	66
TPBT-Br	PTPBTET0.4	PBDBT	−5.65/−3.82	800/873	5.70/1,08	0.900	21.22	55.3	10.56	66
TPBT-Br	PTPBTET0.5	PBDBT	−5.64/−3.84	800/873	6.75/1.14	0.902	18.77	57.5	9.73	66
TPBT-Br	PTPBTET0.75	PBDBT	−5.60/−3.78	800/873	5.10/0.10	0.903	14.50	38.8	5.08	66
Y5-C20-2Br	PYT	PBDBT	−5.56/−3.99	789/854	3.72/5.83	0.88	21.30	62.65	11.75	67
Y5-C20-2Br	PYT-TOE(10)	PBDBT	−5.53/−3.96	789/862	5.14/6.86	0.91	21.57	64.63	12.77	67
Y5-C20-2Br	PYT-TOE(20)	PBDBT	−554/−3.94	790/867	1.80/3.47	0.97	18.75	61.41	10.49	67
Y5-C20-2Br	PYT-TOE(30)	PBDBT	−5.53/−3.96	791/869	0.79/2.26	0.89	16.74	55.01	8.16	67
TPBT-IC	A701 (DIO)	PBDB-T	−5.61/−3.80	−/873	1.24/4.65	0.92	18.27	64	10.70	68
Y5-2BO	P(BDT2BOY5-H)	PBDB-T	−5.60/−4.15	789/855	2.2/4.7	0.92	18.61	51	8.81	69
Y5-2BO	P(BDT2BOY5-F)	PBDB-T	−5.61/−4.16	789/855	2.1/7.6	0.92	19.03	55	9.64	69
Y5-2BO	P(BDT2BOY5-Cl)	PBDB-T	−5.62/−4.18	789/861	2.2/1.4	0.92	18.72	63	11.12	69
Y5	PF5-Y5	PBDB-T	−5.52/−3.84	−/880	0.13/0.076	0.944	20.54	73.1	14.16	34
Y5	PY5-BTZ	PBDB-T	−5.67/−3.72	775/860	0.356/4.83	0.922	22.61	71.1	14.82	70
Y5	PY5−2TZ	PBDB-T	−5.70/−3.76	775/861	0.241/3.43	0.894	20.82	68.4	12.73	70
Y5	PY5-PZ	PBDB-T	−5.71/−3.75	772/856	0.23/2.88	0.893	19.91	68.2	12.10	70
Y5	PY5-BT	PBDB-T	−5.73/−3.78	778/863	0.066/1.02	0.891	15.05	60.4	8.12	70
Y5	PY5-TTz-FT	PBDB-T	−5.70/−3.76	775/861	2.41/3.43	0.894	20.82	68.4	12.73	71
Y5	PY5-TTz-CT	PBDB-T	−5.68/−3.71	790/930	1.74/3.12	0.929	20.44	51.8	9.84	71
TTPBT-ICBr	PBN25-CC	PM6	−5.59/−3.85	792/861	5.45/2.34	0.91	12.40	63.5	7.17	72
TTPBT-ICBr	PBN25	PM6	−5.74/−3.93	799/867	6.37/6.78	0.89	22.62	71.6	14.36	72
Y5	L11	PM6	–	−/892	7.76/4.30	0.95	18.0	64.3	11.1	73
Y5	L14	PM6	−5.76/−3.92	849/892	8.03/6.55	0.953	21.12	71.60	14.41	73
Y5	L15	PM6	−5.75/−3.94	850/898	7.86/6.78	0.953	22.21	71.86	15.22	74
YBO	PFY-DTC	PBDB-T	−5.53/−3.85	−/885	10.1/6.02	0.863	20.20	66.3	12.31	76
YBO	PFY-2TS	PBDB-T	−5.50/−3.85	–	9.78/6.35	0.906	20.47	63.6	11.08	76
Y5-Br	PTH-Y	PBDB-T	−5.55/−3.74	771/850	3.7/0.98	0.956	12.01	57.2	6.57	75
Y5-Br	$PTCl_m$-Y	PBDB-T	−5.60/−3.81	776/866	5.5/1.9	0.941	15.86	55.3	8.25	75
Y5-Br	$PTCl_o$-Y	PBDB-T	−5.61/−3.83	784/870	6.3/3.8	0.948	20.21	66.5	12.74	75
Y5	PYTS-0.0	PBDB-T	−5.88/−4.28	796/879	3.9/0.58	0.92	22.38	63	13.01	77
Y5	PYTS-0.1	PBDB-T	−5.89/−4.94	792/885	3.0/0.98	0.92	22.52	68	14.19	77
Y5	PYTS-0.3	PBDB-T	−5.89/−4.20	793/879	3.4/2.3	0.92	22.91	70	14.68	77
Y5	PYTS-0.5	PBDB-T	−5.88/−4.19	794/885	2.1/0.077	0.92	14.46	60	7.91	77
Y5	PYTS-1.0	PBDB-T	−5.87/−4.17	790/861	3.7/0.0088	0.89	4.31	44	1.71	77
Y5	PYSe	PBDB-T	−5.65/−3.85	804/886	2.33/5.42	0.875	22.79	62.43	12.45	78
Y5	PYSe-TC_6T(10)	PBDB-T	−5.65/−3.83	800/883	3.23/5.01	0.882	22.82	64.29	12.94	78
Y5	PYSe-TC_6T(10)	PBDB-T	−5.62/−3.79	795/873	3.53/5.16	0.891	22.94	66.26	13.54	78
Y5	PYSe-TC_6T(20)	PBDB-T	−5.59/−3.72	792/867	1.46/2.68	0.906	20.08	62.66	11.40	78
Y5-out	Y5-Se-out	PBDB-T	−5.68/−4.24	797/861	2.3/0.45	0.88	16.09	56	7.60	79
Y5-mix	Y5-Se-mix	PBDB-T	−5.68/−4.25	800/867	1.9/0.62	0.89	17.95	58	8.65	79
Y5-in	Y5-Se-in	PBDB-T	−5.68/−4.28	820/885	2.2/1.9	0.86	21.74	72	12.95	79
Y5-out	Y5-BiSe-out	PBDB-T	−5.64/−4.22	792/873	2.0/1.2	0.92	18.12	66	10.13	79
Y5-mix	Y5-BiSe-mix	PBDB-T	−5.64/−4.22	795/873	1.8/0.67	0.92	17.44	60	9.42	79
Y5-in	Y5-BiSe-in	PBDB-T	−5.66/−4.25	800/879	2.0/0.43	0.86	16.54	59	8.31	79
BP2S-ICBr	PFY-0Se	PBDB-T	−5.68/−3.88	800/824	2.76/4.83	0.904	20.9	68.8	13.0	46
BP2S-ICBr	PFY-1Se	PBDB-T	−5.68/−3.89	800/825	2.96/5.51	0.894	21.2	72.9	13.8	46
BP2Se-ICBr	PFY-2Se	PBDB-T	−5.64/−3.91	825/853	3.33/5.85	0.875	23.4	72.0	14.7	46
BP2Se-ICBr	PFY-3Se	PBDB-T	−5.65/−3.92	825/856	3.41/6.23	0.871	23.6	73.7	15.0	46
YN-Br	PYN-BDT	PBDB-T	−5.60/−3.76	822/900	8.84/4.65	0.87	21.33	65	12.06	80
YN-Br	PYN-BDTF	PBDB-T	−5.67/−3.77	–	9.39/5.52	0.86	22.28	69	13.22	80
YN-Br	PYN-BDT	PM6	−5.67/−3.77	–	8.84/3.33	0.97	14.36	52	13.74	80
YN-Br	PYN-BDTF	PM6	−5.67/−3.77	–	8.52/4.05	0.96	16.60	57	9.08	80
–	BTP-T2F	PTQ10	−5.90/−4.03	~750/830	1.75/0.54	0.86	19.58	65.2	11.06	81
–	BTP-2T2F	PTQ10	−5.87/−3.92	~750/839	2.43/1.02	0.89	23.15	69.5	14.32	81
–	RRd-C12	PBDB-T	−5.63/−3.96	793/861	3.4/0.58	0.93	19.14	54	9.39	82
–	RRd-C20	PBDB-T	−0.5.66/3.96	790/861	2.8/0.81	0.93	19.67	63	11.59	82
–	RRd-C24	PBDB-T	−5.68/−3.99	790/849	4.1/1.3	0.93	20.34	67	12.18	82
–	RRg-C20	PBDB-T	−5.66/−3.95	817/879	3.1/3.7	0.88	23.54	73	15.12	82

https://doi.org/10.1021/acsenergylett.2c01541
ACS Energy Lett. 2022, 7, 3835−3854

Table 1. continued

SMA	polymer acceptor	polymer donor	PA HOMO/LUMO (eV)	λ_{peak} (nm)[a] max/onset	μ_h/μ_e (10^{-4} cm^2 V^{-1} s^{-1})[b]	V_{oc} (V)	J_{sc} (mA cm^{-2})	FF (%)	PCE (%)	ref
–	RRg-C24	PBDB-T	−5.68/−3.93	811/873	3.6/4.5	0.88	21.67	71	13.53	82
–	PYDT-2F	PM6	−5.65/−3.90	767/∼899	−/2.40	0.935	24.11	72.08	16.25	83
–	PYDT-3F	PM6	−5.67/−3.94	774/∼905	−/5.02	0.923	24.49	77.01	17.41	83
–	PYDT-4F	PM6	−5.68/−3.96	776/∼912	−/5.54	0.915	24.37	75.20	16.77	83

[a] λ_{peak} is the onset of acceptor film absorption edge. [b] μ_h and μ_e are the hole and electron mobilities of the blend film, respectively.

In brief, Y-series-based polymer acceptors have been mainly developed using two types of A′-cores: BT and BTA. Compared to the BT-based polymer acceptor with high mobility and electronegativity, the BTA core-based polymer acceptor has a higher-lying LUMO level and can improve molecular packing through an additional *N*-alkyl chain. Thus, it is recognized as a promising material which can be applied to all-PSCs.

One of the criteria for main-chain engineering in these polymer acceptors is the chemical modification surrounding the central core. To improve the electron delocalization, polarizability, and quinoidal contribution, Jen et al. found that the replacement of thiophene with selenophene in the Y-series-based polymer main chain reduced the band gap, down-shifted the LUMO level, and enhanced the maximum extinction coefficient of the resulting polymer acceptors.[52] Compared to the devices using selenophene-free analog PYT-2S and symmetrical selenophene-fused analog PYT-2Se, those based on PM6 and PYT-1S1Se with an asymmetrical selenophene-fused backbone (Figure 2) demonstrated an optimized J_{sc} of 24.1 mA cm^{-2} while still maintained a good V_{oc} of 0.926 V owing to their low E_{loss} of 0.502 eV, resulting in a superior PCE of 16.3% (Table 1).

Modifying the end groups of the SMA analog affected the photovoltaic performance because they affected the electron transport via molecular stacking. Accordingly, the modification of the end group influenced the energy levels, absorption, blend morphology, push−pull effect, charge carrier mobility, and photo-stability. The main-chain engineering of the polymer acceptors involving modifications to the end group of the SMA analog could be carried out in diverse ways, including halogenation, regioregularity, and conjugation extension, which were all common techniques. Other ideas involving the combined effect of the end-group modification and side-/main-chain engineering were also considered. As a result, the current study focused primarily on the incorporation of fluorine atoms into the end group of SMA. In this regard, Ying et al. reported fluorinated polymer acceptor PFA1 and discovered that the optimized binary device of PTzBI-*o*F:PFA1 had a PCE value of 15.11%, which was significantly higher than that of PTzBI-*o*F:PY5T (PCE = 4.01%) (Figure 2 and Table 1).[53] In addition to the red-shifted absorption spectra and varying energy levels, the enhanced performance was a result of uniform lamellar chain stacking and miscibility with PTzBI-*o*F. Moreover, PFA1 exhibited excellent device performance with widely used polymer donors (PTzBI-Si, PM6, and PBDBT).

Yan et al. developed PYF-T, a fluorinated polymer acceptor with a different alkyl chain than PFA1 (Figure 2). Two polymer acceptors, PM6:PYF-T and PM6:PY-T (non-fluorinated analog of PYF-T), show different energy level offsets from PM6, but the corresponding all-PSCs display similar V_{oc} values. This is due to the trade-off phenomenon between radiative and non-radiative recombination after fluorination on the end group moiety.[54] A high PCE of 14.10% was reported with the PM6:PYF-T-based device, which is superior to that of the PM6:PY-T-based device (Table 1). By synthesizing PAL1 with two fluorine atoms at the end group (Figure 2) and PAL2 with fluorine atoms at the π-linker (see Figure 3), Lu et al. compared the device performances of two fluorinated polymer acceptors.[55] Both polymers exhibited comparable maximum absorption wavelengths and electronic energy levels. However, the PCE value of the PM6:PAL1-based device was 13.53% (Table 1), higher than that of the PM6:PAL2-based device (9.16%). Owing to the superior molecular planarity, uniform morphology, and tight $\pi-\pi$ stacking, polymer acceptors with fluorinated end groups provided longer carrier lifetime, enhanced charge dissociation, and suppressed charge recombination.

1.1.3. Regioregular End Group. Due to the irregularity at the end group of the SMA analog, the polymer acceptors synthesized from those SMAs were characterized by low crystallinity, weak intermolecular interactions, and low electron mobility. However, these restrictions could be circumvented by producing the polymer acceptors from the monomers with uniformly brominated end groups. Yang et al. reported PY-IT and PY-OT, two well-defined regioregular polymer acceptors (Figure 2).[56] To compare the effect of the polymerization site, a random terpolymer (PY-IOT) comprising two polymer acceptors in equal proportions was developed (Figure 2). Among them, the PM6:PY-IT-based device exhibited a high PCE of 15.05%, J_{sc} of 22.30 mA cm^{-2}, V_{oc} of 0.933 V, and FF of 72.3% (Table 1). Thus, the regioregularity at the end group significantly improved the device performance of PM6:PY-IT relative to other materials.

To investigate the molecular weight effect in regioregular isomers, Yang et al. reported the series polymer acceptor (a regioregular isomer of PJ1) comprising PA-6 (e.g., PA-6-L (8.9 kDa), PA-6-M (12.5 kDa), and PA-6-H (30.1 kDa)), as shown in Figure 2.[44] The binary devices of JD40:PA-6-M and JD40:PA-6-L showed high PCEs of 14.99% and 14.81%, respectively, due to their interconnected fibrillar crystalline morphology. In contrast, the JD40:PA-6-H-based device was manufactured using chlorobenzene and exhibited a low PCE of 12.78% (Table 1). Considering the independent effect of chemical modification and regioregularity at the end group of SMA on the photovoltaic properties of Y-series-based polymer acceptors, it would be worthwhile to examine the combined effect of these modifications in the polymer acceptor's main chain.

Min et al. reported a series of polymer acceptors with thiophene-fused end group acceptors, PYTT-1, PYTT-2, and PYTT-3 (Figure 2),[57] and investigated the degradation of PSCs derived from this polymer series.[58] By using different isomerized thiophene-fused end group, the push−pull behavior, intermolecular interaction, and molecular aggregation of the polymer acceptors can be manipulated. Since

https://doi.org/10.1021/acsenergylett.2c01541
ACS Energy Lett. 2022, 7, 3835−3854

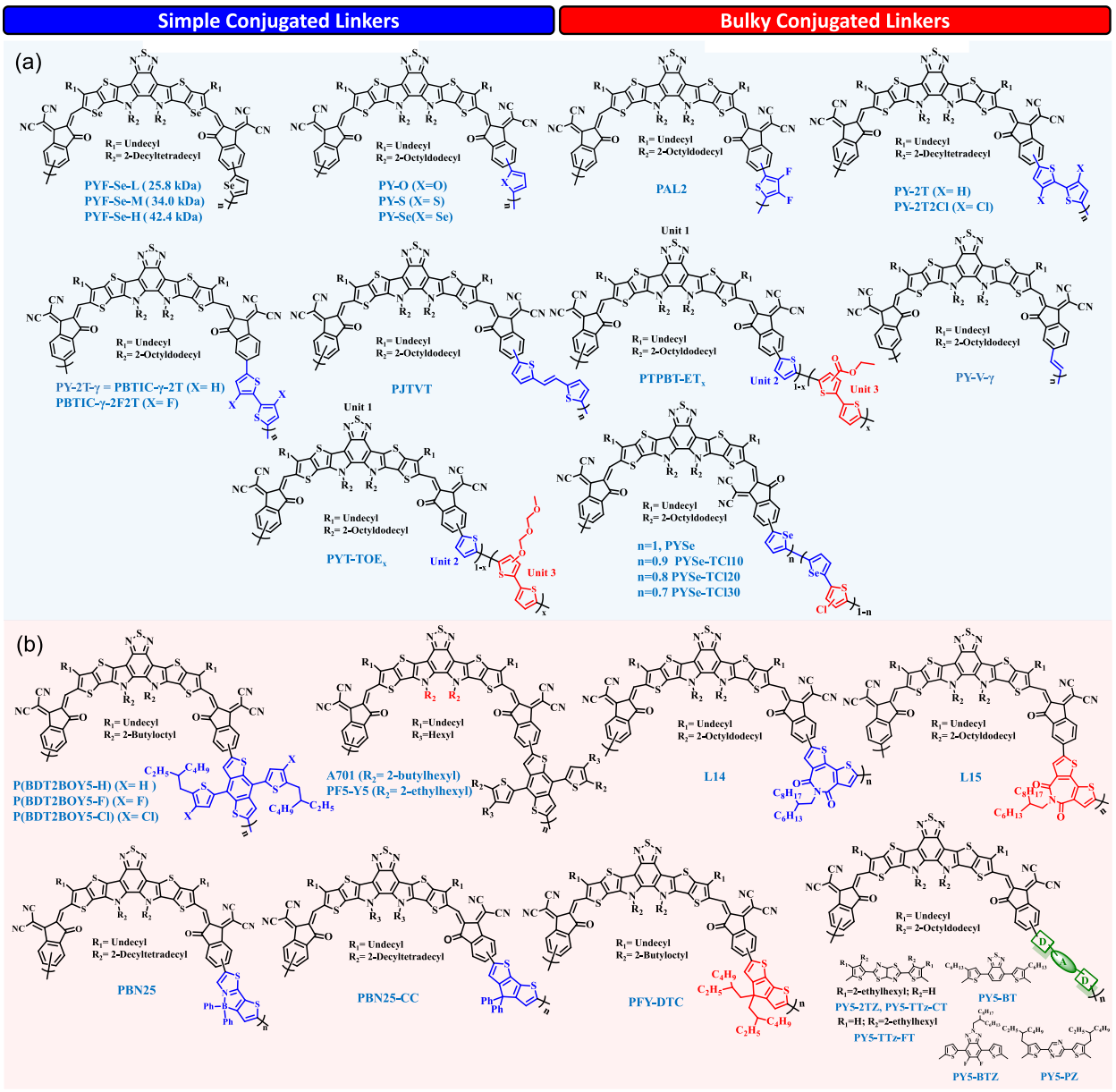

Figure 3. Structures of various polymer acceptors containing (a) simple and (b) bulky conjugated linkers.

PYTT-2 has an intermediate crystallinity between PYTT-1 and PYTT-3, it showed an optimized morphology on the blend film. The device using this polymer showed efficient charge carrier generation and transport properties, yielding an excellent and stable PCE of 14.3% (Table 1).

The regioregularity was also investigated using polymer acceptors composed of SMA with fluorinated end groups. Thus, Yan et al. fabricated two regioregular polymer acceptors, PYF-T-*o* and PYF-T-*m*, comprising SMA analogs with the fluorine atom in the ortho and meta positions to the polymerization site, respectively (Figure 2), and compared their device performances with that of the non-regular polymer acceptor, PYF-T.[45] PM6:PYF-T-*o*-based devices outperformed those of the other acceptors with a PCE value of 15.2% (Table 1). Meanwhile, the small dipole moment of PYF-T-*m* weakened its intramolecular-charge-transfer (ICT) effect and the weak conjugation reduced its light absorptivity and steric hindrance, leading to large crystalline domain size. The PCE value of PYF-T-*m*-based all-PSCs drastically decreased to only 1.4%.

After establishing the superiority of ortho-based regioregular polymer acceptor, the same group compared the device performance of regioregular isomer PY2F-T with two fluorine atoms at the end group of the SMA analog to PYF-T (mono-fluorinated) and PY-T (non-fluorinated) (Figure 2).[59] The PM6:PY2F-T device exhibited a superior PCE value of 15.22% (Table 1) as a result of the fluorine substitution-enhanced ICT effect, as indicated by the red-shifted absorption spectra, tight inter-layer packing, and uniform blend morphology.

1.1.4. Additional Core Design Strategies. Multiple strategies can be applied to simultaneously manipulate the DA′D core and the end group. Jen et al. reported polymer acceptors PY2Se-F and PY2Se-Cl with a selenophene-fused central core and an end group appended with a halogen at the ortho position to the polymerization site in order to study the synergistic effect of all types of modification strategies in the main chain (Figure 2).[60] It was discovered that the

https://doi.org/10.1021/acsenergylett.2c01541
ACS Energy Lett. 2022, 7, 3835−3854

incorporation of halogen and Se improved the crystallinity, interlayer packing, morphology, and charge carrier mobilities in PY2Se-F and PY2Se-Cl compared to those of PY2S-F and non-fluorinated PY2S-H without selenium (Figure 2). The PM6:PY2Se-Cl- and PM6:PY2Se-F-based devices exhibited PCEs of 16.1% and 15.6%, respectively, which were superior to those of the selenium-free PY2S-F- and non-fluorinated PY2S-H-based devices (Table 1).

1.2. Linker Design Strategies. *1.2.1. Simple Conjugated Linkers.* In addition to modifying the core structure of SMA analog, the diversity of linking units is one of the simplest ways to modulate the interlayer packing, improve ICT, expand the absorption range, and enhance the charge carrier transport by introducing the heteroatoms and increasing the conjugation around small thiophene-based linkers. Thus, Min et al. demonstrated a series of polymer acceptors named PY-O, PY-S, and PY-Se synthesized using electron linkers such as furan (O), thiophene (S), and selenophene (Se), respectively, to explore the effect of varying the chalcogen atom in the linker (Figure 3).[61] The optimized photovoltaic parameters of PBDB-T:PY-Se were found to be superior to those of PBDB-T:PY-S and PBDB-T:PY-O, with a PCE of 15.48% (Table 1). This is due to improved interlayer interactions from oxygen to selenium leading to high and balanced charge transport properties. Moreover, owing to the improved miscibility of polymer donor and polymer acceptor and their chain entanglement, the PY-S- and PY-Se-based films exhibited superior photo-stability and mechanical endurance, as evidenced by the high crack-onset-strain (COS) value (>8.70%), high toughness (>2.22 J m^{-3}), and high tensile strength (>28.83 MPa).

Considering the impact of halogenation on the end group of the SMA analog in the preceding sections, it would be worthwhile to examine the insertion of halogen atoms into the linking units. Yuan et al. presented the PY-2T and PY-2T2Cl polymer acceptors that were synthesized by copolymerizing Y5-SMA with bithiophene and chlorinated bithiophene, respectively (Figure 3).[62] A study on the PBDB-T:PY-2T2Cl-based optimal device revealed a PCE value of 9.35% (Table 1), which is superior to PY-2T-based devices. This superiority may be attributed to chlorination at the π-linker, which improved the crystallinity of PY-2T2Cl. In addition, He et al. found that the polymer acceptor PBTIC-γ-2F2T with fluorinated 2,2′-bithiophene as the linker exhibited significantly better absorption properties than PBTIC-γ-2T with non-fluorinated 2,2′-bithiophene as the linker (Figure 3).[63] This superior performance could be attributed to the enhanced J_{sc} value from 20.85 to 22.56 mA cm^{-2} owing to the significant increase of charge carrier mobility with inter-chain packing via F···S interactions of PBTIC-γ-2F2T. Although the HOMO and LUMO energy levels of PBTIC-γ-2F2T were deeper than those of PBTIC-γ-2T, the V_{oc} value of 0.95 V was maintained owing to the lower energy loss of PM6:PBTIC-γ-2F2T device. As a result, the PM6:PBTIC-γ-2F2T-based device exhibited a higher PCE of 14.34%, compared to that of 11.92% for the PM6:PBTIC-γ-2T-based device (Table 1).

To reduce the "randomness" and molecular twisting in the Y-series-based polymer acceptor, Yan et al. utilized a vinylene structure with center of symmetry as the linking unit to design the polymer acceptor PY-V-γ (Figure 3).[64] PY-V-γ exhibited a more ordered coplanar backbone and tighter packing than the PY-T-γ (Figure 2) and PY-2T-γ (Figure 3) with thiophene and bithiophene as linkers, respectively. Consequently, PM6:PY-V-γ-based binary all-PSC attained a PCE of 17.1% with a high J_{sc} of 24.8 mA cm^{-2} and FF of 75.8% (Table 1). Meanwhile, thienylene−vinylene−thienylene (TVT) unit was also known as a conjugated linker useful in organic semiconductor design. Huang et al. demonstrated that TVT conjugated linker is superior to thienylene−ethyl−thienylene (TET) non-conjugated linker.[65] With a PCE of 16.13%, the JD40:PJTVT device performance was superior than that of PJTET (Figure 3 and Table 1). This is due to the incorporation of a conjugated linker that enhanced the planarity, $\pi-\pi$ stacking distance, and delocalization of electrons in PJTVT, thereby facilitating vertical charge transport, electron mobility, and exciton dissociation.

Li et al. used the terpolymer synthetic strategy to construct a new polymer acceptor PTPBT-ET_x, where x denotes the composition of the third component unit, i.e., the 3-ethylesterthiophene (ET) unit, in order to incorporate the two types of small linkers into a Y-series-based polymer acceptor (Figure 3).[66] Replacing PTPBT with PTPBT-$ET_{0.3}$ in devices enhanced the PCE values from 9.96% to 12.52% (Table 1). In addition, the presence of additional S···O interactions in PTPBT-$ET_{0.3}$ decreased the $\pi-\pi$ stacking distance and improved the morphology, thereby enhancing electron and hole mobility and improving J_{sc} and FF in the corresponding device. Using similar strategy, Chen et al. developed another terpolymer acceptor, PYT-TOE(x), by fusing TOE into PYT (where x represents the fraction of thiophene appended to oligoethylene oxide (TOE) as a side chain) (Figure 3).[67] An increase in the proportion of TOE in PYT correlates with a rise in HOMO−LUMO levels, an increase in solubility, and compatibility with PBDB-T. Thus, all photovoltaic parameters in PBDB-T:PYT-TOE(10) were superior to PBDB-T:PYT, which has a PCE of 12.77% (Table 1).

1.2.2. Bulky Conjugated Linkers. In addition to the thiophene-based linkers, numerous complex and extensive structures had been employed as the linking monomers for the Y-series-based polymer acceptors. The Y-series-based polymer acceptors were synthesized using BDT-based linkers, which was structurally similar to the repeating units in the polymer donor, PBDB-T, to enhance the miscibility of the active layer blend. Zhou et al. reported the polymer acceptor, named A701, with BDT as the bulky electron-donating linker (Figure 3).[68] The PBDB-T:A701-based all-PSCs resulted in a PCE value of 10.7%, with V_{oc} and J_{sc} values of 0.92 V and 18.27 mA cm^{-2}, respectively (Table 1). Kim et al. additionally incorporated the halogen atom into the BDT linker and developed the series of polymer acceptors designated P(BDT2BOY5-X), where X = H, F, Cl (Figure 3). With the addition of halogen, P(BDT2BOY5-F) and P(BDT2BOY5-Cl) exhibited a red-shift in their absorption spectra relative to P(BDT2BOY5-H) due to an increase in intermolecular interaction.[69] Among them, the P(BDT2BOY5-Cl)-based device exhibited higher PCE value of 11.2% (Table 1), which is due to the balance of hole/electron mobilities and decreased charge recombination. The all-PSC also exhibited much better thermal stability compared to SMA-based PSC, as the P(BDT2BOY5-Cl)-based device retained 90% of its initial PCE after aging at 100 °C for 100 h. As another example, Wang et al. reported the polymer acceptor PF5-Y5, which was synthesized by modifying the alkyl chain on the BDT linking unit (Figure 3).[34] Compared to the Y5 SMA, the upshifted LUMO level of PF5-Y5 enabled a high V_{oc} of 0.944 V for the corresponding all-PSC. Owing to the

https://doi.org/10.1021/acsenergylett.2c01541
ACS Energy Lett. 2022, 7, 3835−3854

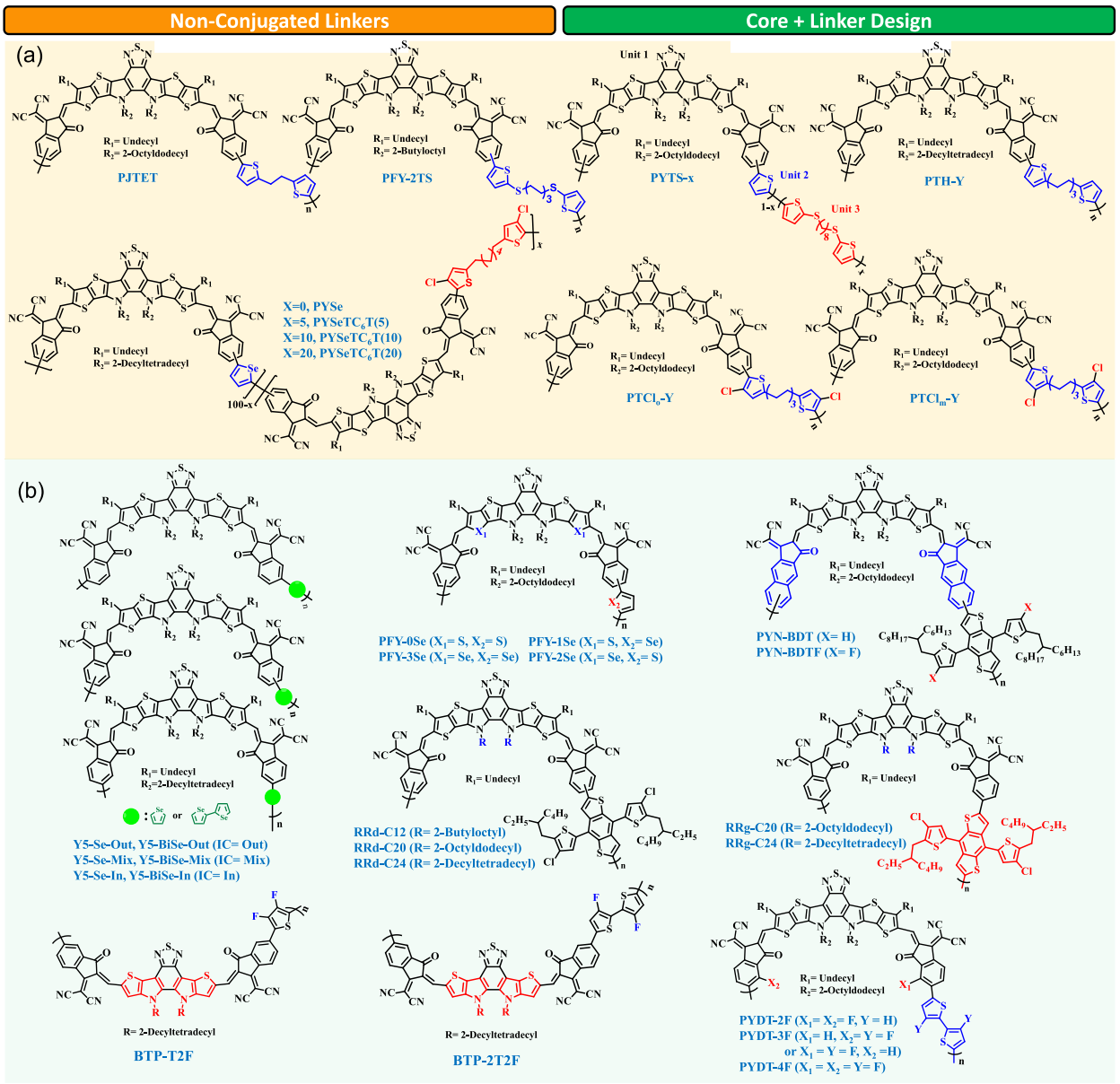

Figure 4. (a) Polymer acceptors containing non-conjugated linkers. (b) Polymer acceptors designed by combination of core and linker engineering.

improved V_{oc} and the reduced energy loss, the device based on PBDB-T:PF5-Y5 exhibited a high PCE value of 14.16% (Table 1).

The introduction of a D-A-D acceptor moiety as a linkage unit to the Y-series-based polymer acceptors could lower energy levels and create additional channels for the electron transport. For example, Li et al. developed a series of polymer acceptors, i.e., PY5-BTZ (benzotriazole), PY5-2TZ (thiazolothiazole), PY5-PZ (pyrazine), and PY5-BT (benzothiadiazole), in the order of increasing acceptor strength of D-A-D-type linker, to construct polymer acceptors with a narrow band gap (Figure 3).[70] Among these, PBDB-T:PY5-BTZ has absorption spectra in the range 700−900 nm with a strong absorption coefficient and outperforms other acceptors with a PCE of 14.82% (Table 1). The same group also synthesized PY5-TTz-FT and PY5-TTz-CT, two polymer acceptors with isomerized D-A-D-type linking units containing ethylhexyl side chains (Figure 3).[71] PY5-TTz-FT exhibited a PCE value of 12.73% (Table 1), which is superior to that of PY5-TTz-CT due to more efficient exciton dissociation, bimolecular recombination, and charge transport. This study suggested that the position of the side chain on the D-A-D linker unit played an important role in manipulating the energy levels of the polymer acceptor, as well as the molecular packing for an ideal interpenetrating network between donor and acceptor polymer chains.

Considering the device performances of Y-series-based polymer acceptors with electron-donating and D-A-D-type linkers, it would be worthwhile to examine their device efficiency by selecting an electron-deficient linker to enhance n-type characteristics. Thus, Liu et al. synthesized the polymer acceptor PBN25 by incorporating an electron-deficient boron−nitrogen coordination bond (B←N) into the linking unit (Figure 3). The PM6:PBN25-based all-PSC demonstrated a PCE of 14.3%, which is superior to the device of PM6:PBN25-CC without the (B←N) unit (Figure 3 and Table 1).[72] The increase in PCE value was attributed to the

https://doi.org/10.1021/acsenergylett.2c01541
ACS Energy Lett. 2022, 7, 3835−3854

fact that the insertion of (B←N) lowered the HOMO levels of the acceptor, which promoted photo-induced hole transfer from the polymer acceptor to the polymer donor. Guo et al. reported the narrow band gap polymer acceptor L14 with the electron-deficient linker bithiophene imide (BTI) (Figure 3).[73] In comparison to L11 (Figure 2), L14 exhibited superior light-harvesting properties and down-shifted energy levels. In addition, the PCE value of PM6:L14-based all-PSCs was 14.3%. Due to the larger energy offset of L14 with PM6 and low energy loss, this device displayed a considerably higher V_{oc} of 0.96 V than PM6:L11. Moreover, the device performance was enhanced by synthesizing the regioregular isomer of L14, i.e., L15 (Figure 3), and the PCE value was increased to 15.22% (Table 1).[74]

1.2.3. Non-conjugated Linkers. The simplest way to create flexible Y-series-based polymer acceptors is to replace the conjugated linkers with non-conjugated linkers, which reduces the backbone rigidity while maintaining the high thermal stabilities of the active layers. The introduction of such flexible linkers adds some degrees of conformational freedom and energetic disorder. Although this appears to have a negative effect on the electronic properties of polymer acceptors, it is considered to improve the polymer miscibility, processability, and mechanical stability. For instance, Chen et al. developed PTCl$_m$-Y and PTCl$_o$-Y polymer acceptors by utilizing the position isomers of chlorinated non-conjugated linkers (Figure 4).[75] The PBDB-T:PTCl$_o$-Y-based all-PSCs device exhibited a PCE value that was 12.74%, higher than those of its positional isomer, PTCl$_m$-Y, and non-chlorinated analog, PTH-Y (Table 1). This was due to the tight $\pi-\pi$ stacking and uniform surface morphology of PBDB-T:PTCl$_o$-Y, which facilitated charge transport, balanced charge carrier mobility, reduced trap-assisted recombination, and improved the photovoltaic parameters. More importantly, the PCE was maintained 85% after 1000 cycles (bending radius = 4 mm), with no obvious crack in the PBDB-T:PTCl$_o$-Y active layer. In another study, a polymer acceptor structure using thioalkyl bithiophene was also introduced. Wang et al. also developed the polymer acceptor PFY-2TS with a flexible thioalkyl bithiophene (2TS) linker and compared its photovoltaic properties to those of the polymer acceptor PFY-DTC (Figure 4).[76] The PBDB-T:PFY-2TS-based device displayed a PCE of 12.31%, with a lower value of energy loss of 0.56 eV (Table 1). PFY-2TS exhibited superior miscibility with PBDB-T, leading to a smaller domain size due to the non-conjugated linker, outperforming PFY-DTC.

To combine the advantages of conjugated and non-conjugated linkers in a Y-series-based polymer acceptor, Wang et al. reported the terpolymer PYTS-x with various compositions of linking units such as thiophene and TS8 non-conjugated linker (Figure 4).[77] The PBDB-T:PYTS-0.3-based device displayed the highest PCE of 14.68% (Table 1) due to its superior crystallinity and charge carrier mobility. Noticeably, excellent mechanical stretchability was obtained, with a COS of 21.64% and toughness of 3.86 MJ m^{-3}, which is a great enhancement compared to the devices based on the fully conjugated polymer acceptor. Chen et al. employed the same strategy, with selenophene as the conjugated linker and chlorinated 1,6-di(thiophen-2-yl)hexane (TC$_6$T) as the non-conjugated linker in a terpolymer structure, PYSe-TC$_6$T(x).[78] The incorporation of a non-conjugated linker up-shifted the LUMO level and decreased the aggregation and crystallinity of the terpolymer acceptor, while simultaneously enhancing the donor:acceptor miscibility. By balancing the ratio between conjugated and non-conjugated units, the PSC device with PBDB-T:PYSe-TC$_6$T(10) exhibited a higher PCE of 13.54% than the PSC device with a fully conjugated polymer acceptor (Table 1). The good miscibility of PBDB-T:PYSe-TC$_6$T(10) also improved the blade-coated film quality, resulting in an outstanding PCE of 11.96% for the large-area (1.21 cm^2) device.

1.3. Combined Effects of Core and Linker. To design the Y-series-based polymer acceptors, it would be benign to investigate the combined effects of core and linker engineering after comprehending their respective functions. In this context, Kim et al. examined the effects of the molecular structure of the end group of the SMA analog, as well as the modifications of linker units.[79] Incorporating selenophene or biselenophene as the linker with different positional isomeric monomers resulted in the Y5-Se and Y5-BiSe series of polymer acceptors (i.e., Y5-Se-In, Y5-Se-Out, and Y5-Se-mix, and Y5-BiSe-In, Y5-BiSe-Out, and Y5-BiSe-Mix, respectively, Figure 4). Due to its high absorption coefficient and electron mobility, Y5-Se-In exhibited the highest PCE value of 13.38% in the Y5-Se series. When biselenophene was used as the linker, however, Y5-BiSe-Out achieved the highest PCE value of 10.67% (Table 1). To explain this opposite trend, it was found that Y5-Se-In and Y5-BiSe-Out have a more planar conformation and tighter chain packing than other polymeric isomers.

By manipulating the linker structure and regioregularity of the Y-series-based monomer, it is possible to alter the performance of all-PSCs. Further, Jen et al. studied the combined effect of modifications of the main chain and linking units, resulting in the development of PFY-0Se, PFY-1Se, PFY-2Se, and PFY-3Se, all of which contain selenophene in their central core and linking unit (Figure 4).[46] Moreover, PBDB-T:PFY-3Se-based devices with a medium M_n value (M_n = 34.0 kDa) demonstrated superior device performance with a PCE value of 15.1% compared to PFY-Se devices with a low or high M_n value (Table 1).

Marks et al. also reported polymer acceptors with π-extended end groups, namely PYN-BDT and PYN-BDTF, by employing BDT and fluorinated BDT as linkers, respectively (Figure 4).[80] All-PSCs were produced by combining PBDB-T or PM6 with PYN-BDT or PYN-BDTF acceptor polymer. Among them, the conventional device based on PBDB-T:PYN-BDTF exhibited the highest PCE of 13.22%. The reasons for PBDB-T:PYN-BDTF-based all-PSC's superior performance are as follows: (i) an increase in the conjugation of end groups decreased the optical band gap (1.38 eV) and (ii) the presence of fluorine played a role in reducing the $\pi-\pi$ stacking distance. As another strategy to improve device efficiency, Peng et al. modified the structure of the acceptor by removing two fused thiophene rings from the native DA′D core and developed two polymer acceptors with different linking units, BTP-T2F and BTP-2T2F (Figure 4).[81] The BTP-2T2F:PTQ10-based device exhibited a high PCE of 14.32%, which is superior to the PTQ10:BTP-T2F-based device. Due to the higher LUMO level and extinction coefficient of BTP-2T2F, having an additional thiophene ring in the linker unit, the former binary device exhibited relatively high values of J_{sc} and V_{oc}. In addition, examples of improving device performance by controlling the regularity in the polymer structure were also presented. Kim et al. developed a series of regioregular polymer acceptors called RRg-24 (2-decyltetradecyl) and RRg-20 (2-octyldodecyl) and compared their device performances

https://doi.org/10.1021/acsenergylett.2c01541
ACS Energy Lett. 2022, 7, 3835−3854

with those of regiorandom isomers called RRd-C12 (2-butyloctyl), RRd-C20 (2-octydodecyl), and RRd-C24 (2-decyltetradecyl) (Figure 4).[82] PBDB-T:RRg-24 and PBDB-T:RRg-20 exhibited minimizing molecular defects and balanced hole mobility/electron mobility (μ_h/μ_e) values, i.e., 0.8, with superior device performances with PCEs of 13.53−15.12% compared to the devices with RRd series.

Another design strategy involves the halogenation on both the core and linker moieties. Peng et al. demonstrated three Y-series-based polymer acceptors, PYDT-2F, PYDT-3F, and PYDT-4F, with varying numbers of fluorine atoms on the end groups and bithiophene linkers.[83] With the increasing of the number of fluorine substituent, narrow optical band gap, down-shifted HOMO level, reduced surface energy, and enhanced miscibility with the fluorinated donor polymer PM6 could be achieved. Especially, all-PSC based on PM6:PYDT-3F exhibited a maximum PCE of 17.41% with a high FF of 77.01% owing to the deep HOMO level of PM6 and the favorable morphology of the blend film.To create advanced Y-series-based polymer acceptors with excellent power conversion efficiency values of binary and non-binary all-polymer solar cells, a simultaneous investigation must be conducted on the Y-series-based small-molecule acceptors and linkers.

To create advanced Y-series-based polymer acceptors with excellent power conversion efficiency values of binary and non-binary all-polymer solar cells, a simultaneous investigation must be conducted on the Y-series-based small-molecule acceptors and linkers.

Multiple factors, such as regioregularity, side chains, and the insertion of heterogeneous atoms, can alter the properties of the polymer acceptors, as demonstrated by the examples presented previously. To create advanced Y-series-based polymer acceptors with excellent PCE values, a simultaneous investigation must be conducted on the Y-series-based SMA and linkers. Therefore, chemical structure modification strategies, such as alkylation, fused-core/end group engineering involving the insertion of chalcogen and halogen atoms, change in the conjugation length, variation in conjugation, flexibility, and the electronic nature of the linking unit, as discussed above, should be considered judiciously and require further investigation to increase the PCE of all-PSCs to 20% and beyond.

2. POLYMER ACCEPTORS FOR NON-BINARY ACTIVE LAYER

Despite the inspiring progress made in the binary all-PSCs with the Y-series-based polymer acceptors through various molecular engineering strategies, the efficiency of all-PSCs still needs to be enhanced. Due to the thermodynamically unfavorable mixing of the polymer donors and polymer acceptors, the binary all-PSCs have intrinsically poor morphologies and insufficient stabilities.[84] In terms of device engineering, a non-binary active layer capable of producing a robust and durable all-PSC using the Y-series polymer acceptor was therefore considered. It was developed by (i) ternary strategy, i.e., the addition of a third component, which could improve the miscibility of host materials while reducing the carrier recombination losses and enhancing the stability, and (ii) single-component strategy with a single polymer material in the photoactive layer.

2.1. Ternary Blend Strategy. *2.1.1. Fullerene Derivative as a Third Component.* As previously discussed, the PM6:PY-IT-based binary device exhibited a PCE of 14.84%. Thus, a fullerene derivative can be added as an additive to achieve high device performance and mechanical stability for practical applications. Primarily, Tao et al. observed that the small energy offset between the HOMO and LUMO of PY-IT (Figure 2) and those of PM6 resulted in limited charge transport, leading to low J_{sc} value for the corresponding device.[85] Consequently, they found that the addition of $PC_{71}BM$ (Figure 5) with a deep HOMO level enhanced the performance of the device by realizing a HOMO energy level cascade. The PM6:PY-IT:$PC_{71}BM$ ternary system demonstrated improved V_{oc}, J_{sc}, and FF with a PCE value of 16.36% (Table 2). Similarly, the PCE value of PM6:PY-IT was improved to 16.16% by using a low-cost "technical grade" PCBM, i.e., incompletely separated blends of $PC_{61}BM$ and $PC_{71}BM$ (Figure 5), as a compatibilizer to improve the active layer morphology.[86] The V_{oc}, J_{sc}, and FF of the ternary-based devices were increased to 0.956 V, 22.93 mA cm^{-2}, and 73.6%, respectively (Table 2). Moreover, the small amount of technical grade-PCBM disrupted the formation of large polymer crystallites and PCBM aggregates, thus enhancing mechanical endurance of the ternary blend film with a COS value of 11.1%. Further, Huang et al. developed the ternary system by integrating 1% of $PC_{71}BM$ as an additive into the binary blend of PTzBI-*o*F:PFA1.[87] It was discovered that the processing with $PC_{71}BM$ did not contribute to the absorption but decrease the large-scale phase separation of PTzBI-*o*F:PFA1 blend film. Hence, PTzBI-*o*F:PFA1:$PC_{71}BM$ (1:1:0.01)-based device showed relatively high PCE of 15.6% (Table 2), so as to weaken carrier recombination and improve the FF.

2.1.2. Polymer Acceptor as a Third Component. Despite the high charge carrier mobility of fullerene derivatives, it is advisable to use non-fullerene polymer additives to improve the miscibility and long-term stability of the all-PSCs. Thus, Yan et al. improved the device performance of PM6:PY-IT by incorporating BN-T (Figure 4), a non-fullerene polymer acceptor with B←N-type electron-deficient structural units.[88] The ternary system composed of PM6:PY-IT:BN-T (1:1:0.1) exhibited a PCE of 16.09% higher than PM6:PY-IT (Table 2) due to the occurrence of both charge and energy transfer between the two polymer acceptors, PY-T and BN-T. The addition of BN-T also improved the shelf-life and photostability of the devices, and >90% of the initial PCEs of BN-T-containing all-PSCs were maintained even after storing for 10 days or light-soaking for 116 h (1 sun condition). Another example can be found in the work of Yang et al., where they chose N2200 (Figure 5) as an additive to the binary blend of PM6:PY-IT to broaden the absorption spectra of the blend film.[89] In the presence of 0.7 vol% CN and 3 wt% N2200, a high PCE of 16.04% was obtained (Table 2). Similarly, Guo et al. chose the MBTI polymer acceptor as the third component that can achieve complementary absorption spectra to efficiently transfer energy to L15 (Figure 5).[74] By facilitating the effective charge generation between a polymer donor and polymer acceptor, the PCE value of the resultant ternary system (PM6:L15:MBTI) was increased to 16.18% (Table 2)

https://doi.org/10.1021/acsenergylett.2c01541
ACS Energy Lett. 2022, 7, 3835−3854

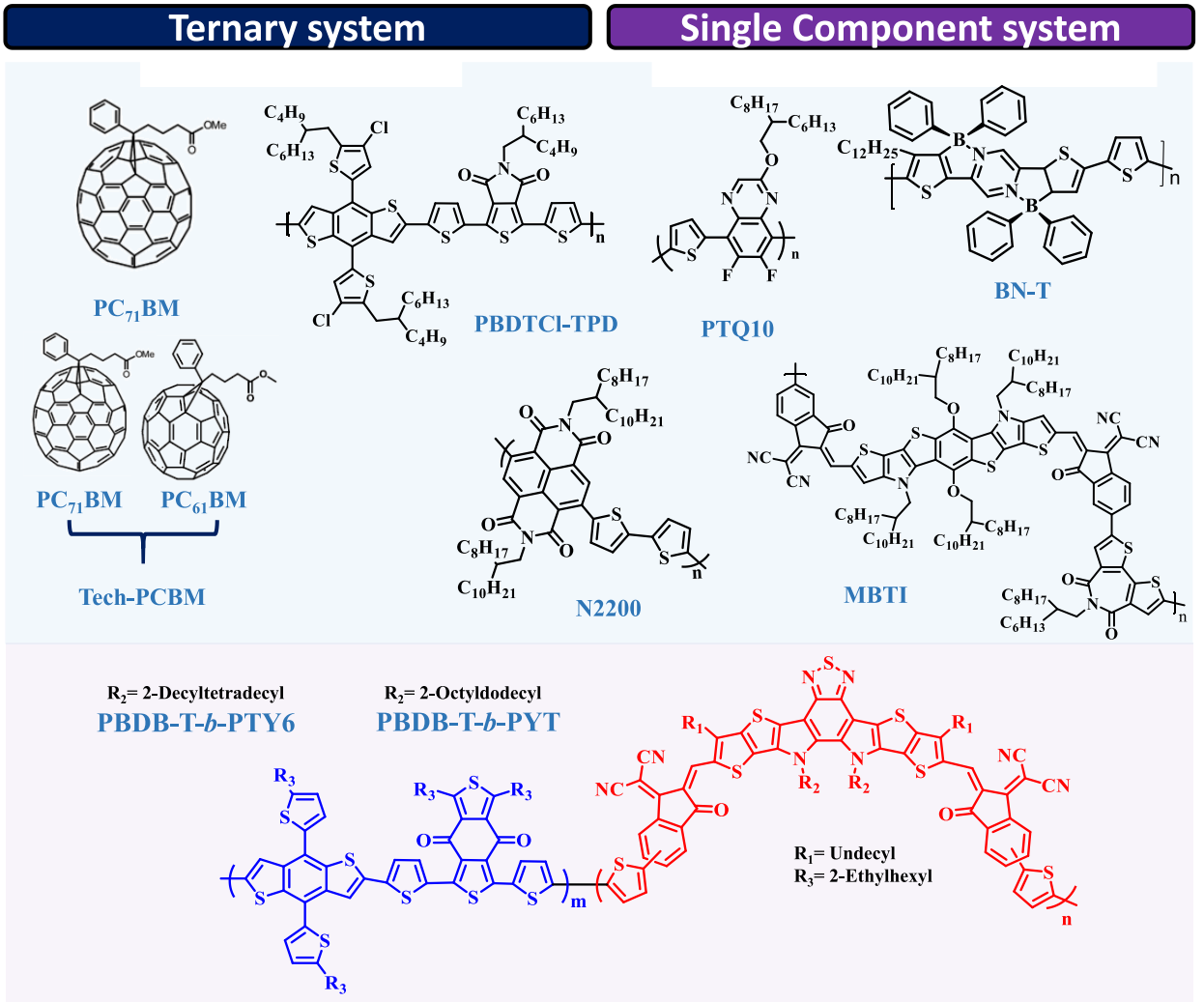

Figure 5. Ternary and single-component systems involving Y-series-based polymer acceptors.

compared to that of PM6:L15-based binary system (15.22%) (previously discussed in section 1.2.2).

To ensure compatibility between the acceptors, the third component can be a polymer acceptor based on the Y-series. Li et al. synthesized PYCl-T, a chlorinated Y-series-based polymer acceptor (Figure 2), and incorporated it into PM6:PY-IT blends.[90] Thus, the addition of PYCl-T permits the realization of cascade energy alignment and the formation of a bicontinuous fibrillar interpenetration network in the ternary blend films. Despite a slight decrease in the V_{oc} due to the low LUMO of PYCl-T, J_{sc} and FF of the ternary-blend-based PSC were improved, resulting in a higher PCE of 16.62% compared to those of the binary PSCs (Table 2). Utilizing terpolymer PYSe-TCl20 (Figure 3) and polymer acceptor PTCl$_o$-Y (Figure 4) with non-conjugated linkages, Chen et al. demonstrated the significance of D:A:A′-type ternary systems.[91] The PCE value of the ternary blend of PBDB-T:PYSe-TCl20:PTCl$_o$-Y-based all-PSCs was 15.26%. These findings demonstrated that the collaborative effect of terpolymerization with a non-conjugated backbone and a ternary system can effectively regulate the morphology of blends and improve the performance of the device. Previously discussed in section 1.1.3, the binary device based on PM6:PY2F-T had a maximum PCE of 15.0%, which is superior to that of PM6:PYT (non-fluorinated polymer acceptors) with a PCE of 14.5%.[31] Hence, Min et al. developed an efficient ternary system based on PM6:PYT:PY2F-T by considering a proper energy-transfer mechanism.[92] They demonstrated that an increase in J_{sc} value from 21.3 mA cm^{-2} to 24.2 mA cm^{-2} was the sole cause of this improvement, with a trade-off with V_{oc} (from 0.96 to 0.87 V) and energy loss (0.46 to 0.50 eV) values due to larger energy offsets between PY2F-T and PM6. The PM6:PYT:PY2F-T-based ternary system achieved the high PCE of 17.2% (Table 2), together with improved light-soaking and photo-thermal stability compared to the binary devices.

2.1.3. Polymer Donor as a Third Component. Polymer donors can also be used as the third component to realize D:D′:A-type (two donors:one acceptor) ternary systems. For example, Li et al. selected PTQ10 with complementary absorption spectra, compatibility, and lower HOMO energy levels relative to PBDB-T.[86] Consequently, the PBDB-T:PTQ10:PTPBT-ET0.1 (1.3:0.2:1) system (Figure 5) exhibited a PCE value of 14.56%, which is superior to those of PBDB-T:PTPBT-ET0.1 (13.63%) and PTQ10:PTPBT-ET0.1 (3.15%) (Table 2). Later, the same group continued to use PTQ10 as the third component to the PM6:PY-IT binary blend, which increased the PCE to 16.52% for the PM6:PTQ10:PY-IT (1.0:0.2:1.0) device (Table 2).[94] V_{oc} and J_{sc} of the ternary-based PSCs were enhanced due to the down-

https://doi.org/10.1021/acsenergylett.2c01541
ACS Energy Lett. 2022, 7, 3835−3854

Table 2. Photovoltaic Parameters of the All-PSCs Non-binary Systems

Ternary Systems								
binary components	third component/additive	ratio	μ_h/μ_e (10^{-4} cm^2 V^{-1} s^{-1})[b]	V_{oc} (V)	J_{sc} (mA cm^{-2})	FF (%)	PCE (%)	ref
PM6:PY-IT	$PC_{71}BM$	–	6.75/6.32	0.942	25.06	69.27	16.36	85
PM6:PY-IT	Tech-$PC_{71}BM$	1:0.8:0.2	1.55/1.70	0.956	22.93	73.6	16.16	86
PM6:PY-IT	BN-T	1:1:0	8.61/4.763	0.937	21.90	73.6	15.11	88
PM6:PY-IT	BN-T	1:1:0.1	9.98/5.87	0.955	22.65	74.3	16.09	88
PM6:PY-IT	BN-T	1:1:0.2	9.68/4.98	0.958	22.46	72.0	15.51	88
PM6:PY-IT	N2200 + CN	–	8.79/5.22	0.947	22.60	74.9	16.04	89
PM6:PY-IT	PYCl-T	1:1:0.2	5.79/6.27	0.913	24.3	73.40	16.3	90
PM6: PY-IT	PTQ10	1:0.2:1	7.86/6.81	0.94	23.79	73.87	16.52	94
PBDB-T:PYSe-TC120	PTCl*o*-Y	1:1.1:0.1	5.83/3.12	0.91	23.18	72.1	15.26	91
PTzBI-*o*F:PFA1	–	–	0.174/0.042	0.86	24.3	67.2	14.6	87
PTzBI-*o*F:PFA1	$PC_{71}BM$	1:1:0.01	0.235/0.171	0.86	24.5	73.1	15.6	87
PM6:L15	MBTI	1:1:0.05	8.15/7.81	0.957	22.91	73.83	16.18	74
PM6: PY2F-T	PYT	1:1.2:0.3	6.88/6.56	0.90	25.2	76.0	17.2	92
PBDB-T:PTPBT-ET0.1	PTQ10	1.5:0:1	–	0.888	23.15	66.31	13.63	93
PBDB-T:PTPBT-ET0.1	PTQ10	1.3:0.2:1	4.68/3.36	0.909	23.68	67.64	14.56	93
PBDB-T:PTPBT-ET0.1	PTQ10	1:0.5:1	–	0.912	22.20	67.86	13.74	93
PBDB-T:PTPBT-ET0.1	PTQ10	0.75:0.75:1	–	0.916	21.51	65.18	12.84	93
PBDB-T:PTPBT-ET0.1	PTQ10	0:1.5:1	–	0.972	6.48	50.03	3.15	93
PTQ10:BTP-2T2F	PBDTCl-TPD	0.8:0.2:1.2	–	0.89	23.49	72.3	15.12	81
PTQ10:BTP-2T2F	PBDTCl-TPD	0.6:0.4:1	2.26/8.34	0.89	23.91	75.4	16.04	81
PTQ10:BTP-2T2F	PBDTCl-TPD	0.4:0.6:1.2	–	0.88	23.56	72.8	15.09	81
PTQ10:BTP-2T2F	PBDTCl-TPD	0.2:0.8:1.2	–	0.88	22.92	70.6	14.24	81

Single-Component Systems									
single-component system (SCS)	acceptor block/ donor block	HOMO/LUMO (eV)	λ_{peak} (nm)[a] max/ onset	μ_h/μ_e (10^{-4} cm^2 V^{-1} s^{-1})[b]	V_{oc} (V)	J_{sc} (mA cm^{-2})	FF (%)	PCE (%)	ref
PBDB-T-*b*-PTY6	PTY6/PBDB-T	−5.50/−3.67	600−800	1.54/0.64	0.89	15.42	63	8.64	95
PBDB-T-*b*-PYT (chloroform)	PYT/PBDB-T	−5.38/−3.67	700−800	3.62/3.46	0.916	19.6	63	11.32	96
PBDB-T-*b*-PYT (*o*-silene)	PYT/PBDB-T	–	–	3.64/3.28	0.895	20.57	68.46	12.60	97

[a] λ_{peak} is the onset of acceptor film absorption edge. [b] μ_h and μ_e are the hole and electron mobilities of the blend film, respectively.

shifted HOMO levels of PTQ10 (Figure 4) compared to those of PBDB-T and PM6. With PTQ10 as the host donor, Peng et al. reported that the incorporation of PBDTCl-TPD polymer donor (Figure 5) improved the PCE of the PTQ10:BTP-2T2F binary device (PCE = 14.32%, previously discussed in section 1.3) to 16.04% (PTQ10:PBDTCl-TPD:BTP-2T2F = 0.6:0.4:1.2) (Table 2).[81] Moreover, the addition of PBDTCl-TPD improved polymer miscibility, crystallization, and consequently, device performance.

With the PCEs exceeding 17%, ternary PSCs systems with the polymer acceptors based on the Y-series have generated exciting opportunities in this promising field. Therefore, the judicious choice of the third component in the design of the successful ternary all-PSCs can generate a PCE of 20% or more in the future.

2.2. Single-Component Strategy. After observing the remarkable device performances of Y-series-based polymer acceptors in binary and ternary component systems, the feasibility of using Y-series-based single-component OPVs to achieve sufficient stability and device performance for practical implementation must be examined. Ma et al. adopted the Y-series and ITIC-based polymer acceptors and the PBDB-T polymer donor to design the block copolymers PBDB-T-*b*-PTY6 (Figure 5) and PBDB-T-*b*-PIDIC2T, respectively, for the development of an efficient single-component-based device.[95] Due to the high electron affinity of Y-series-based polymer acceptor, PBDB-T-*b*-PTY6 produced a PCE of 8.64%, higher than that of PBDB-T-*b*-PIDIC2T (4.20%) (Table 2). More importantly, the PBDB-T-*b*-PTY6-based OPV maintained more than 80% of its initial PCE after aging at 80 °C for over 1000 h, which is a significant improvement from the corresponding binary device. Independently, Min et al. also reported a Y-series-based block copolymer, PBDB-T-*b*-PYT, (Figure 5) with slightly shorter alkyl side chains than PBDB-T-*b*-PTY6. The PBDB-T-*b*-PYT device displayed a remarkable PCE of 11.32% (Table 2).[96] Despite the fact that the PCE of PBDB-T-*b*-PYT-based devices lags behind those of PBDB-T:PYT binary devices, their lower non-radiative energy loss and superior long-term stabilities once again demonstrate the superiority of single-component devices.[97] With *o*-xylene as the solvent, a PCE of 12.60% was obtained for PBDB-T-*b*-PYT device, which is the highest PCE value ever observed in a single-component system to date (Table 2).

Thus, the ternary strategy has demonstrated its efficacy in terms of the device performance with a variety of third components for the complementary absorption, cascade energy level alignment, and morphological enhancement. The importance of simple fabrication and durability in the single-component devices, thus, makes the OPV devices practical.- With the end goal of commercialization in mind, more effort should be devoted to improving the device's stability rather than simply increasing the power conversion efficiency.

https://doi.org/10.1021/acsenergylett.2c01541
ACS Energy Lett. 2022, 7, 3835−3854

With the end goal of commercialization in mind, more effort should be devoted to improving the device's stability rather than simply increasing the power conversion efficiency.

3. SUMMARY AND OUTLOOK

The recent development of high-performance all-PSCs with Y-series-based polymer acceptors in binary and non-binary systems demonstrated that all-PSCs containing polymer acceptors based on the Y-series possess all the benefits associated with SMAs as well as additional remarkable properties. By taking advantage of the A-DA′D-A structure with excellent synthetic flexibility of the Y-series-based structures as well as multiple possible combination with different linkers, various strategies have been utilized to narrow the PCE gap between all-PSCs and SMA-based PSCs. The main-chain backbone with electron-withdrawing end groups exhibits planar geometry that is associated with the efficient intramolecular charge transport and molecular packing for achieving higher electron transporting ability. The suitable design of linkers is helpful for efficient intermolecular charge transport and controlled molecular aggregation. Thus, all-PSCs involving Y-series-based polymer acceptors displayed broad absorption spectra (300−950 nm) and low band gaps. The present review showed the attractive features of the all-PSCs based on Y-series-based polymer acceptors in terms of reducing energy losses around 0.49 eV for high V_{oc}, suppressing unfavorable carrier recombination losses and charge-transfer states for high J_{sc}, and morphology optimization to ensure a high FF. Due to the above-discussed superior features, the highest PCE of 18% was eventually achieved in all-PSCs involving Y-series-based polymer acceptors. In the coming years, it can be expected that these devices will be able to compete with SMA-based devices. Despite these remarkable achievements in all-PSCs, the batch-to-batch variations, solubility, purity, and large-scale production of the conjugated polymer acceptors are still quite challenging. The following strategies are proposed to further improve device performance for potential future applications of this technology based on the disclosed working mechanism:

(1) Until now, the vast majority of publications have mostly described the use of a PBDB-T polymer donor or its fluorinated derivative PM6 in conjunction with Y-series-based polymer acceptors. New polymer or small-molecule donors with complementary absorptions, suitable energy levels, crystallinity, and miscibility with Y-series-based polymer acceptors should be designed to simultaneously improve the V_{oc}, J_{sc}, and FF of the resulting PSCs. To acquire high-performance D-A copolymer donors, the development of acceptor moieties based on quinoxaline (PBQx-H-TF and PQM-Cl)[98,35] or imide (PTzBI-*o*F and Q4)[53,99] has been proven a feasible method. The Same-A-Strategy using BT moieties (D18 and JD40)[100,101] can be applied to ensure good miscibility between polymer donors and Y-series-based polymer acceptors. In addition, the synthesis of high-performance polymer donors with simple structure, such as PTQ10,[81] is crucial to reduce the fabrication cost. Small-molecule donors (Se-1 and Se-2)[102] are also good candidates in the blend with Y-series-based polymer acceptors.

(2) New Y-series-based polymer acceptors could be developed by selecting a new conjugated core with intermediate electron affinity to increase the absorption range for high-performance flexible devices. Simple aromatic all-fused rings[103] or unfused backbones with non-covalent interactions, such as S···N, F···H, or O···H,[104−106] can be incorporated into the design of new polymer acceptors to reduce production costs and enhance device stability. Highly branched polymer structures have been developed to realize 3D networks with good crystallinity and solubility.[107] Besides, by connecting two SMAs through a π-bridge, the design of A-π-A (N-π-N) quasi-macromolecule acceptors[108,109] increases the conjugation length for more electron delocalization while still maintaining definite molecular structures with fewer chain entanglements. Consequently, it is possible to simultaneously achieve the high device performance of SMA-based PSCs and the excellent device stability observed with all-PSCs.

(3) As previous research has demonstrated that the high PCE values in both PSCs with SMAs (>19%) and polymer acceptors (>17%) were obtained with ternary systems, more effort can be devoted to this category. The ternary strategy should be capable of stabilizing the binary counterparts by improving the morphology and enhancing the hydrophobicity. From a review of the relevant literature, we can hypothesize that regioregular and fluorinated Y-series-based polymer acceptors, as well as SMAs as a third component, can balance the phase separation and crystallization properties, thereby increasing the charge carrier mobility, FF, and J_{sc} values of the corresponding PSCs.

(4) In addition to the design and synthesis of new photoactive materials, the structure and fabrication of PSC devices also play significant roles. In addition to the conventional BHJ structure with donor:acceptor blends, quasi-planar heterojunctions (Q-PHJs),[110] or interdigitated heterojunctions (IHJs)[111] can be realized by sequential deposition[112−114] to control the microstructure of the active layer and improve the device PCE.

(5) In terms of simple processes, researchers should concentrate on single-component PSCs by synthesizing Y-series-based block copolymers and double-cable polymers; these PSCs offer superior photo- and thermal stability as well as mechanical robustness compared to binary blend-based PSCs for both outdoor and indoor photovoltaics. The introduction of Y-series-based polymer acceptor into single-component PSCs will be advantageous due to their strong absorption in the NIR region and high electron mobility. We believe that the strong electronegativity of the Y-series acceptor moiety will emphasize the ICT characteristics of the excited state upon coupling with certain p-type polymer donors and will provide balanced energy levels and charge transport, thus providing the benefit of high J_{sc} values.

(6) To compete with inorganic solar cells, it is desirable to utilize the high viscoelasticity and high absorption coefficient of polymer acceptors in lightweight, flexible devices. With the end goal of commercialization in mind, more effort should be devoted to improving the device's stability rather than simply increasing the PCE.

https://doi.org/10.1021/acsenergylett.2c01541
ACS Energy Lett. 2022, 7, 3835−3854

Consideration may be given to the development of stable materials and the application of device encapsulation, inverted structure, or cross-linking strategies of active layer. Indoor applications should also be prioritized, as organic materials have the unique ability to match their absorption spectra to different light sources.

AUTHOR INFORMATION

Corresponding Authors

Min Ju Cho − *Department of Chemistry, Research Institute for Natural Sciences, Korea University, Seoul 02841, Republic of Korea*; Email: chominju@korea.ac.kr

Dong Hoon Choi − *Department of Chemistry, Research Institute for Natural Sciences, Korea University, Seoul 02841, Republic of Korea*; orcid.org/0000-0002-3165-0597; Email: dhchoi8803@korea.ac.kr

Authors

Meenal Kataria − *Department of Chemistry, Research Institute for Natural Sciences, Korea University, Seoul 02841, Republic of Korea*

Hong Diem Chau − *Department of Chemistry, Research Institute for Natural Sciences, Korea University, Seoul 02841, Republic of Korea*

Na Yeon Kwon − *Department of Chemistry, Research Institute for Natural Sciences, Korea University, Seoul 02841, Republic of Korea*

Su Hong Park − *Department of Chemistry, Research Institute for Natural Sciences, Korea University, Seoul 02841, Republic of Korea*

Complete contact information is available at: https://pubs.acs.org/10.1021/acsenergylett.2c01541

Author Contributions

‡M.K. and H.D.C. contributed equally to this work.

Notes

The authors declare no competing financial interest.

Biographies

Meenal Kataria is presently working as a research professor in the field of optoelectronics with Prof. Dong Hoon Choi's research group at Korea University, Seoul. She completed her Ph.D. in 2019 at the Guru Nanak Dev University, Punjab, India. Her current research interests focus on the design and synthesis of organic semiconductors for organic photovoltaics.

Hong Diem Chau received her M.Sc. degree from HCMC University of Education, Vietnam, in 2017. She is now a Ph.D. student at Korea University under the supervision of Prof. Dong Hoon Choi. Her research interests focus on the synthesis of organic photovoltaic materials and the characterization of devices.

Na Yeon Kwon is a Ph.D. student studying under the guidance of Prof. Dong Hoon Choi, Department of Chemistry, Korea University. Her current research interests are designing and synthesizing organic semiconductors for organic optoelectronic applications, such as active materials for organic light-emitting diodes and photovoltaic cells.

Su Hong Park is a Ph.D. student studying under the supervision of Prof. Dong Hoon Choi, Department of Chemistry, Korea University. He is currently conducting research on synthesizing organic materials required for active materials for organic light-emitting diodes and photovoltaic cells and applying them to related devices.

Min Ju Cho received his Ph.D. from Korea University in 2009. He served as postdoctoral fellow at the State University of New York at Buffalo from 2009 to 2012. He is currently a research professor in the Research Institute for Natural Sciences in Korea University.

Dong Hoon Choi received his Ph.D. from the University of Michigan in Ann Arbor, Michigan, USA, in 1991. He became a Professor of Chemistry at Korea University in 2005 and is currently a fellow at the Korean Academy of Science and Technology. His main research interests are organic semiconducting materials.

ACKNOWLEDGMENTS

The authors acknowledge financial support from the National Research Foundation of Korea (NRF-2019R1A6A1-A11044070, 2020R1I1A1A01066897, and 2022R1A2B5-B02001454).

REFERENCES

(1) Li, Z.; Liang, Y.; Qian, X.; Ying, L.; Cao, Y. Conquering the Morphology Barrier of Ternary All-Polymer Solar Cells by Designing Random Terpolymer for Constructing Efficient Binary All-Polymer Solar Cells. *Chem. Eng. J.* **2022**, *439*, 135491.

(2) Zhang, Y. Z.; Wang, N.; Wang, Y. H.; Miao, J. H.; Liu, J.; Wang, L. X. 15% Efficiency All-Polymer Solar Cells Based on a Polymer Acceptor Containing B← N Unit. *Chin. J. Polym. Sci.* **2022**, *40*, 989−995.

(3) Fan, B.; Zhong, W.; Ying, L.; Zhang, D.; Li, M.; Lin, Y.; Xia, R.; Liu, F.; Yip, H.-L.; Li, N.; Ma, Y.; Brabec, C. J.; Huang, F.; Cao, Y. Surpassing the 10% Efficiency Milestone for 1-cm^2 All-Polymer Solar Cells. *Nat. Commun.* **2019**, *10*, 4100.

(4) Meng, Y.; Wu, J.; Guo, X.; Su, W.; Zhu, L.; Fang, J.; Zhang, Z.-G.; Liu, F.; Zhang, M.; Russell, T. P.; Li, Y. 11.2% Efficiency All-Polymer Solar Cells with High Open-Circuit Voltage. *Sci. China Chem.* **2019**, *62*, 845−850.

(5) Gu, X.; Wei, Y.; Liu, X.; Yu, N.; Li, L.; Han, Z.; Gao, J.; Li, C.; Wei, Z.; Tang, Z.; Zhang, X.; Huang, H. (2022). Low-cost Polymer Acceptors with Noncovalently Fused-Ring Backbones for Efficient All-Polymer Solar Cells. *Sci. China Chem.* **2022**, *65*, 926−933.

(6) Yue, Y.; Zheng, B.; Yang, W.; Huo, L.; Wang, J.; Jiang, L. Meniscus-Assisted Coating with Optimized Active-Layer Morphology toward Highly Efficient All-Polymer Solar Cells. *Adv. Mater.* **2022**, *34*, 2108508.

(7) Wu, Y.; Schneider, S.; Walter, C.; Chowdhury, A. H.; Bahrami, B.; Wu, H.-C.; Qiao, Q.; Toney, M. F.; Bao, Z. Fine-Tuning Semiconducting Polymer Self-Aggregation and Crystallinity Enables Optimal Morphology and High-Performance Printed All-Polymer Solar Cells. *J. Am. Chem. Soc.* **2020**, *142*, 392−406.

(8) Zhu, L.; Zhong, W.; Qiu, C.; Lyu, B.; Zhou, Z.; Zhang, M.; Song, J.; Xu, J.; Wang, J.; Ali, J.; Feng, W.; Shi, Z.; Gu, X.; Ying, L.; Zhang, Y.; Liu, F. Aggregation-Induced Multilength Scaled Morphology Enabling 11.76% Efficiency in All-Polymer Solar Cells Using Printing Fabrication. *Adv. Mater.* **2019**, *31* (41), 1902899.

(9) Liu, X.; Zhang, C.; Pang, S.; Li, N.; Brabec, C. J.; Duan, C.; Huang, F.; Cao, Y. Ternary All-Polymer Solar Cells With 8.5% Power Conversion Efficiency and Excellent Thermal Stability. *Front. Chem.* **2020**, *8*, 302.

(10) Li, Z.; Ying, L.; Zhu, P.; Zhong, W.; Li, N.; Liu, F.; Huang, F.; Cao, Y. A Generic Green Solvent Concept Boosting the Power Conversion Efficiency of All-Polymer Solar Cells to 11%. *Energy Environ. Sci.* **2019**, *12*, 157−163.

(11) Kim, M.; Kim, H. I.; Ryu, S. U.; Son, S. Y.; Park, S. A.; Khan, N.; Shin, W. S.; Song, C. E.; Park, T. Improving the Photovoltaic Performance and Mechanical Stability of Flexible All-Polymer Solar Cells via Tailoring Intermolecular Interactions. *Chem. Mater.* **2019**, *31*, 5047−5055.

(12) Kim, A.; Park, C. G.; Park, S. H.; Kim, H. J.; Choi, S.; Kim, Y. U.; Jeong, C. H.; Chae, W. S.; Cho, M. J.; Choi, D. H. Highly Efficient

and Highly Stable Terpolymer-based All-Polymer Solar Cells with Broad Complementary Absorption and Robust Morphology. *J. Mater. Chem. A* **2018**, *6*, 10095−10103.
(13) Li, Z.; Zhang, W.; Xu, X.; Genene, Z.; Di Carlo Rasi, D.; Mammo, W.; Yartsev, A.; Andersson, M. R.; Janssen, R. A.; Wang, E. High-Performance and Stable All-Polymer Solar Cells Using Donor and Acceptor Polymers with Complementary Absorption. *Adv. Energy Mater.* **2017**, *7*, 1602722.
(14) Zhang, Z.-G.; Yang, Y.; Yao, J.; Xue, L.; Chen, S.; Li, X.; Morrison, W.; Yang, C.; Li, Y. Constructing a Strongly Absorbing Low-Bandgap Polymer Acceptor for High-Performance All-Polymer Solar Cells. *Angew. Chem., Int. Ed.* **2017**, *56*, 13503−13507.
(15) Zhang, Q.; Yuan, X.; Feng, Y.; Larson, B. W.; Su, G. M.; Maung Maung, Y.; Rujisamphan, N.; Li, Y.; Yuan, J.; Ma, W. Understanding the Interplay of Transport-Morphology-Performance in PBDB-T-Based Polymer Solar Cells. *Sol. RRL* **2020**, *4*, 1900524.
(16) Guo, Y.; Li, Y.; Awartani, O.; Han, H.; Zhao, J.; Ade, H.; Yan, H.; Zhao, D. Improved Performance of All-Polymer Solar Cells Enabled by Naphthodiperylenetetraimide-Based Polymer Acceptor. *Adv. Mater.* **2017**, *29*, 1700309.
(17) Long, X.; Ding, Z.; Dou, C.; Zhang, J.; Liu, J.; Wang, L. Polymer Acceptor Based on Double B←N Bridged Bipyridine (BNBP) Unit for High-Efficiency All-Polymer Solar Cells. *Adv. Mater.* **2016**, *28*, 6504−6508.
(18) Yao, H.; Bai, F.; Hu, H.; Arunagiri, L.; Zhang, J.; Chen, Y.; Yu, H.; Chen, S.; Liu, T.; Lai, Y.; Zou, J. Y. L.; Ade, H.; Yan, H. Efficient All-Polymer Solar Cells based on a New Polymer Acceptor Achieving 10.3% Power Conversion Efficiency. *ACS Energy Lett.* **2019**, *4*, 417−422.
(19) Wu, J.; Meng, Y.; Guo, X.; Zhu, L.; Liu, F.; Zhang, M. All-Polymer Solar Cells based on a Novel Narrow-Bandgap Polymer Acceptor with Power Conversion Efficiency over 10%. *J. Mater. Chem. A* **2019**, *7*, 16190−16196.
(20) Yao, H.; Ma, L.-K.; Yu, H.; Yu, J.; Chow, P. C. Y.; Xue, W.; Zou, X.; Chen, Y.; Liang, J.; Arunagiri, L.; Gao, F.; Sun, H.; Zhang, G.; Ma, W.; Yan, H. All-Polymer Solar Cells with over 12% Efficiency and a Small Voltage Loss Enabled by a Polymer Acceptor Based on an Extended Fused Ring Core. *Adv. Energy Mater.* **2020**, *10*, 2001408.
(21) Fan, Q.; Su, W.; Chen, S.; Kim, W.; Chen, X.; Lee, B.; Liu, T.; Méndez-Romero, U. A.; Ma, R.; Yang, T.; Zhuang, W.; Li, Y.; Li, Y.; Kim, T.-S.; Hou, L.; Yang, C.; Yan, H.; Yu, D.; Wang, E. Mechanically Robust All-Polymer Solar Cells from Narrow Band Gap Acceptors with Hetero-Bridging Atoms. *Joule* **2020**, *4*, 658−672.
(22) Li, Y.; Jia, Z.; Zhang, Q.; Wu, Z.; Qin, H.; Yang, J.; Wen, S.; Woo, H. Y.; Ma, W.; Yang, R.; Yuan, J. Toward Efficient All-Polymer Solar Cells via Halogenation on Polymer Acceptors. *ACS Appl. Mater. Interfaces* **2020**, *12*, 33028−33038.
(23) Feng, L.; Yuan, J.; Zhang, Z.; Peng, H.; Zhang, Z. G.; Xu, S.; Liu, Y.; Li, Y.; Zou, Y. Thieno [3,2-b] pyrrolo-fused Pentacyclic Benzotriazole-based Acceptor for Efficient Organic Photovoltaics. *ACS Appl. Mater. Interfaces* **2017**, *9* (37), 31985−31992.
(24) Yuan, J.; Huang, T.; Cheng, P.; Zou, Y.; Zhang, H.; Yang, J. L.; Chang, S. Y.; Zhang, Z.; Huang, W.; Wang, R.; Meng, D.; Gao, F.; Yang, Y. Enabling Low Voltage Losses and High Photocurrent in Fullerene-Free Organic Photovoltaics. *Nat. Commun.* **2019**, *10*, 570.
(25) Wang, R.; Yuan, J.; Wang, R.; Han, G.; Huang, T.; Huang, W.; Xue, J.; Wang, H. C.; Zhang, C.; Zhu, C.; Cheng, P.; Meng, D.; Yi, Y.; Wei, K.-H.; Zou, Y.; Yang, Y. Rational Tuning of Molecular Interaction and Energy Level Alignment Enables High-Performance Organic Photovoltaics. *Adv. Mater.* **2019**, *31* (43), 1904215.
(26) Wang, H. C.; Chen, C. H.; Li, R. H.; Lin, Y. C.; Tsao, C. S.; Chang, B.; Tan, S.; Yang, Y.; Wei, K. H. Engineering the Core Units of Small-Molecule Acceptors to Enhance the Performance of Organic Photovoltaics. *Sol. RRL* **2020**, *4* (10), 2000253.
(27) Yuan, J.; Zhang, Y.; Zhou, L.; Zhang, G.; Yip, H. L.; Lau, T. K.; Lu, X.; Zhu, C.; Peng, H.; Johnson, P. A.; Leclerc, M.; Cao, Y.; Ulanski, J.; Li, Y.; Zou, Y. Single-Junction Organic Solar Cell with over 15% Efficiency Using Fused-Ring Acceptor with Electron-Deficient Core. *Joule* **2019**, *3*, 1140−1151.
(28) Zhao, W.; Li, S.; Yao, H.; Zhang, S.; Zhang, Y.; Yang, B.; Hou, J. Molecular Optimization Enables over 13% Efficiency in Organic Solar Cells. *J. Am. Chem. Soc.* **2017**, *139*, 7148−7151.
(29) Li, S.; Ye, L.; Zhao, W.; Zhang, S.; Mukherjee, S.; Ade, H.; Hou, J. Energy-Level Modulation of Small-Molecule Electron Acceptors to Achieve over 12% Efficiency in Polymer Solar Cells. *Adv. Mater.* **2016**, *28*, 9423−9429.
(30) Lin, Y.; Wang, J.; Zhang, Z. G.; Bai, H.; Li, Y.; Zhu, D.; Zhan, X. An Electron Acceptor Challenging Fullerenes for Efficient Polymer Solar Cells. *Adv. Mater.* **2015**, *27*, 1170−1174.
(31) Lin, Y.; He, Q.; Zhao, F.; Huo, L.; Mai, J.; Lu, X.; Su, C. J.; Li, T.; Wang, J.; Zhu, J.; Sun, Y.; Wang, C.; Zhan, X. A Facile Planar Fused-Ring Electron Acceptor for As-Cast Polymer Solar Cells with 8.71% Efficiency. *J. Am. Chem. Soc.* **2016**, *138*, 2973−2976.
(32) Wu, Q.; Wang, W.; Wang, T.; Sun, R.; Guo, J.; Wu, Y.; Jiao, X.; Brabec, C. J.; Li, Y.; Min, J. High-Performance All-Polymer Solar Cells with only 0.47 eV Energy Loss. *Sci. China Chem.* **2020**, *63*, 1449−1460.
(33) Jia, T.; Zhang, J.; Zhong, W.; Liang, Y.; Zhang, K.; Dong, S.; Ying, L.; Liu, F.; Wang, X.; Huang, F.; Cao, Y. 14.4% Efficiency All-polymer Solar Cell with Broad Absorption and Low Energy Loss Enabled by a Novel Polymer Acceptor. *Nano Energy* **2020**, *72*, 104718.
(34) Fan, Q.; An, Q.; Lin, Y.; Xia, Y.; Li, Q.; Zhang, M.; Su, W.; Peng, W.; Zhang, C.; Liu, F.; Hou, L.; Zhu, W.; Yu, D.; Xiao, M.; Moons, E.; Zhang, F.; Anthopoulos, T. D.; Inganas, O.; Wang, E. Over 14% Efficiency All-Polymer Solar Cells Enabled by a Low Bandgap Polymer Acceptor with Low Energy Loss and Efficient Charge Separation. *Energy Environ. Sci.* **2020**, *13*, 5017.
(35) Wang, J.; Cui, Y.; Xu, Y.; Xian, K.; Bi, P.; Chen, Z.; Zhou, K.; Ma, L.; Zhang, T.; Yang, Y.; Zu, Y.; Yao, H.; Hao, X.; Ye, L.; Hou, J. A New Polymer Donor Enables Binary All-Polymer Organic Photovoltaic Cells with 18% Efficiency and Excellent Mechanical Robustness. *Adv. Mater.* **2022**, *34*, 2205009.
(36) Zhu, L.; Zhang, M.; Xu, J.; Li, C.; Yan, J.; Zhou, G.; Zhong, W.; Hao, T.; Song, J.; Xue, X.; Zhou, Z.; Zeng, R.; Zhu, H.; Chen, C.-C.; MacKenzie, R. C. I.; Zou, Y.; Nelson, J.; Zhang, Y.; Sun, Y.; Liu, F. Single-Junction Organic Solar Cells with Over 19% Efficiency Enabled by a Refined Double-Fibril Network Morphology. *Nat. Mater.* **2022**, *21*, 656−663.
(37) Cui, Y.; Xu, Y.; Yao, H.; Bi, P.; Hong, L.; Zhang, J.; Zu, Y.; Zhang, T.; Qin, J.; Ren, J.; Chen, Z.; He, C.; Hao, X.; Wei, Z.; Hou, J. Single-Junction Organic Photovoltaic Cell with 19% Efficiency. *Adv. Mater.* **2021**, *33*, 2102420.
(38) Lee, C.; Lee, S.; Kim, G.-U; Lee, W.; Kim, B. J. Recent Advances, Design Guidelines, and Prospects of All-Polymer Solar Cells. *Chem. Rev.* **2019**, *119*, 8028−8086.
(39) Wang, G.; Melkonyan, F. S.; Facchetti, A.; Marks, T. J. All-Polymer Solar Cells: Recent Progress, Challenges, and Prospects. *Angew. Chem., Int. Ed.* **2019**, *58*, 4129−4142.
(40) Genene, Z.; Mammo, W.; Wang, E.; Andersson, M. R. Recent Advances in n-Type Polymers for All-Polymer Solar Cells. *Adv. Mater.* **2019**, *31*, 1807275.
(41) Zhang, Z.-G.; Li, Y. Polymerized Small-Molecule Acceptors for High-Performance All-Polymer Solar Cells. *Angew. Chem., Int. Ed.* **2021**, *60*, 4422−4433.
(42) Luo, D.; Jang, W.; Babu, D. D.; Kim, M. S.; Wang, D. H.; Kyaw, A. K. K. Recent Progress in Organic Solar Cells Based on Non-Fullerene Acceptors: Materials to Devices. *J. Mater. Chem. A* **2022**, *10*, 3255.
(43) Wang, W.; Wu, Q.; Sun, R.; Guo, J.; Wu, Y.; Shi, M.; Yang, W.; Li, H.; Min, J. Controlling Molecular Mass of Low-Band-Gap Polymer Acceptors for High-Performance All-Polymer Solar Cells. *Joule* **2020**, *4*, 1070−1086.
(44) Jia, J.; Huang, Q.; Jia, T.; Zhang, K.; Zhang, J.; Miao, J.; Huang, F.; Yang, C. Fine-Tuning Batch Factors of Polymer Acceptors Enables a Binary All-Polymer Solar Cell with High Efficiency of 16.11%. *Adv. Energy Mater.* **2022**, *12*, 2103193.

https://doi.org/10.1021/acsenergylett.2c01541
ACS Energy Lett. 2022, 7, 3835−3854

(45) Yu, H.; Pan, M.; Sun, R.; Agunawela, I.; Zhang, J.; Li, Y.; Qi, Z.; Han, H.; Zou, X.; Zhou, W.; Chen, S.; Lai, J. Y. L.; Luo, S.; Luo, Z.; Zhao, D.; Lu, X.; Ade, H.; Huang, F.; Min, J.; Yan, H. Regio-Regular Polymer Acceptors Enabled by Determined Fluorination on End Groups for All-Polymer Solar Cells with 15.2% Efficiency. *Angew. Chem., Int. Ed.* **2021**, *60*, 10137−10146.
(46) Fan, Q.; Fu, H.; Wu, Q.; Wu, Z.; Lin, F.; Zhu, Z.; Min, J.; Woo, H. Y.; Jen, A. K.-Y. Multi-Selenophene-Containing Narrow Bandgap Polymer Acceptors for All-Polymer Solar Cells with over 15% Efficiency and High Reproducibility. *Angew. Chem., Int. Ed.* **2021**, *60*, 15935−15943.
(47) Li, Y.; Song, J.; Dong, Y.; Jin, H.; Xin, J.; Wang, S.; Cai, Y.; Jiang, L.; Ma, W.; Tang, Z.; Sun, Y. Polymerized Small Molecular Acceptor with Branched Side Chains for All Polymer Solar Cells with Efficiency over 16.7%. *Adv. Mater.* **2022**, *34*, 2110155.
(48) Du, J.; Hu, K.; Zhang, J.; Meng, L.; Yue, J.; Angunawela, I.; Yan, H.; Qin, S.; Kong, X.; Zhang, Z.; Guan, B.; Ade, H.; Li, Y. Polymerized Small Molecular Acceptor Based All-Polymer Solar Cells with an Efficiency of 16.16% via Tuning Polymer Blend Morphology by Molecular Design. *Nat. Commun.* **2021**, *12*, 5264.
(49) Fu, H.; Li, Y.; Yu, J.; Wu, Z.; Fan, Q.; Lin, F.; Woo, H. Y.; Gao, F.; Zhu, Z.; Jen, A. K.-Y. High Efficiency (15.8%) All-Polymer Solar Cells Enabled by a Regioregular Narrow Bandgap Polymer Acceptor. *J. Am. Chem. Soc.* **2021**, *143*, 2665−2670.
(50) Zhang, B.; Li, J.; Tang, A.; Geng, Y.; Guo, Q.; Zhou, E. Utilizing Benzotriazole-Fused DAD-Type Heptacyclic Ring to Construct n-Type Polymer for All-Polymer Solar Cell Application. *ACS Appl. Energy Mater.* **2021**, *4*, 4217−4223.
(51) Zhu, C.; Li, Z.; Zhong, W.; Peng, F.; Zeng, Z.; Ying, L.; Huang, F.; Cao, Y. Constructing a new polymer acceptor enabled non-halogenated solvent-processed all-polymer solar cell with an efficiency of 13.8%. *Chem. Commun.* **2021**, *57*, 935−938.
(52) Fu, H.; Fan, Q.; Gao, W.; Oh, J.; Li, Y.; Lin, F.; Qi, F.; Yang, C.; Marks, T. J.; Jen, A. K.-Y. 16.3% Efficiency Binary All-Polymer Solar Cells Enabled by a Novel Polymer Acceptor with an Asymmetrical Selenophene-Fused Backbone. *Sci. China Chem.* **2022**, *65*, 309−317.
(53) Peng, F.; An, K.; Zhong, W.; Li, Z.; Ying, L.; Li, N.; Huang, Z.; Zhu, C.; Fan, B.; Huang, F.; Cao, Y. A Universal Fluorinated Polymer Acceptor Enables All-Polymer Solar Cells with > 15% Efficiency. *ACS Energy Lett.* **2020**, *5*, 3702−3707.
(54) Yu, H.; Qi, Z.; Yu, J.; Xiao, Y.; Sun, R.; Luo, Z.; Cheung, A. M. H.; Zhang, J.; Sun, H.; Zhou, W.; Chen, S.; Guo, X.; Lu, X.; Gao, F.; Min, J.; Yan, H. Fluorinated End Group Enables High-Performance All-Polymer Solar Cells with Near-Infrared Absorption and Enhanced Device Efficiency over 14%. *Adv. Energy Mater.* **2021**, *11*, 2003171.
(55) Yang, Q.; Yu, W.; Lv, J.; Huang, P.; He, G.; Xiao, Z.; Kan, Z.; Lu, S. Effects of Fluorination Position on All-Polymer Organic Solar Cells. *Dyes Pigm.* **2022**, *200*, 110180.
(56) Luo, Z.; Liu, T.; Ma, R.; Xiao, Y.; Zhan, L.; Zhang, G.; Sun, H.; Ni, F.; Chai, G.; Wang, J.; Zhong, C.; Zou, Y.; Guo, X.; Lu, X.; Chen, H.; Yan, H.; Yang, C. Precisely Controlling the Position of Bromine on the End Group Enables Well-Regular Polymer Acceptors for All-Polymer Solar Cells with Efficiencies over 15%. *Adv. Mater.* **2020**, *32*, 2005942.
(57) Wang, T.; Sun, R.; Wang, W.; Li, H.; Wu, Y.; Min, J. Highly Efficient and Stable All-Polymer Solar Cells Enabled by Near-Infrared Isomerized Polymer Acceptors. *Chem. Mater.* **2021**, *33*, 761−773.
(58) Guo, J.; Wang, T.; Wu, Y.; Sun, R.; Wu, Q.; Wang, W.; Wang, H.; Xia, X.; Lu, X.; Wang, T.; Min, J. Revealing the Microstructure-Related Light-Induced Degradation for All-Polymer Solar Cells based on Regioisomerized End-Capping Group Acceptors. *J. Mater. Chem. C* **2022**, *10*, 1246−1258.
(59) Yu, H.; Luo, S.; Sun, R.; Angunawela, I.; Qi, Z.; Peng, Z.; Zhou, W.; Han, H.; Wei, R.; Pan, M.; Cheung, A. M. H.; Zhao, D.; Zhang, J.; Ade, H.; Min, J.; Yan, H. A Difluoro-Monobromo End Group Enables High-Performance Polymer Acceptor and Efficient All-Polymer Solar Cells Processable with Green Solvent under Ambient Condition. *Adv. Funct. Mater.* **2021**, *31*, 2100791.
(60) Fan, Q.; Fu, H.; Luo, Z.; Oh, J.; Fan, B.; Lin, F.; Yang, C.; Jen, A. K.-Y. Near-Infrared Absorbing Polymer Acceptors Enabled by Selenophene-Fused Core and Halogenated End-Group for Binary All-Polymer Solar Cells with Efficiency Over 16%. *Nano Energy* **2022**, *92*, 106718.
(61) Wu, Q.; Wang, W.; Wu, Y.; Sun, R.; Guo, J.; Shi, M.; Min, J. Tailoring polymer Acceptors by Electron Linkers for Achieving Efficient and Stable All-Polymer Solar Cells. *Natl. Sci. Rev.* **2022**, *9*, nwab151.
(62) Li, Y.; Wang, M.; Zhang, Q.; Wu, Z.; Lim, H.; Wang, Y.; Qin, H.; Yang, J.; Gao, C.; Young Woo, H.; Yuan, J. Fine-Tuned Crystallinity of Polymerized Non-Fullerene Acceptor via Molecular Engineering Towards Efficient All-Polymer Solar Cell. *Chem. Eng. J.* **2022**, *428*, 131232.
(63) Wang, H.; Chen, H.; Xie, W.; Lai, H.; Zhao, T.; Zhu, Y.; Chen, L.; Ke, C.; Zheng, N.; He, F. Configurational Isomers Induced Significant Difference in All-Polymer Solar Cells. *Adv. Funct. Mater.* **2021**, *31*, 2100877.
(64) Yu, H.; Wang, Y.; Kim, H. K.; Wu, X.; Li, Y.; Yao, Z.; Pan, M.; Zou, X.; Zhang, J.; Chen, S.; Zhao, D.; Huang, F.; Lu, X.; Zhu, Z.; Yan, H. A Vinylene-Linker-Based Polymer Acceptor Featuring a Coplanar and Rigid Molecular Conformation Enables High-Performance All-Polymer Solar Cells with Over 17% Efficiency. *Adv. Mater.* **2022**, *34*, 2200361.
(65) Zhang, J.; Tan, C.-H.; Zhang, K.; Jia, T.; Cui, Y.; Deng, W.; Liao, X.; Wu, H.; Xu, Q.; Huang, F.; Cao, Y. Extended Conjugated Polymer Acceptor Containing Thienylene−Vinylene−Thienylene Unit for High-Performance Thick-Film All-Polymer Solar Cells with Superior Long-Term Stability. *Adv. Energy Mater.* **2021**, *11*, 2102559.
(66) Du, J.; Hu, K.; Meng, L.; Angunawela, I.; Zhang, J.; Qin, S.; Liebman-Pelaez, A.; Zhu, C.; Zhang, Z.; Ade, H.; Li, Y. High-Performance All-Polymer Solar Cells: Synthesis of Polymer Acceptor by a Random Ternary Copolymerization Strategy. *Angew. Chem., Int. Ed.* **2020**, *59*, 15181−15185.
(67) Wu, F.; Liu, J.; Liu, J.; Oh, J.; Huang, B.; Chen, D.; Liu, Z.; He, Q.; Yang, C.; Chen, L. Thiophene with Oligoethylene Oxide Side Chain Enables Random Terpolymer Acceptor to Achieve Efficient All-Polymer Solar Cells. *ChemElectroChem* **2021**, *8*, 3936−3942.
(68) Tang, A.; Li, J.; Zhang, B.; Peng, J.; Zhou, E. Low-Bandgap n-Type Polymer Based on a Fused-DAD-Type Heptacyclic Ring for All-Polymer Solar Cell Application with a Power Conversion Efficiency of 10.7%. *ACS Macro Lett.* **2020**, *9*, 706−712.
(69) Lee, J.-W.; Sun, C.; Ma, B. S.; Kim, H. J.; Wang, C.; Ryu, J. M.; Lim, C.; Kim, T.-S.; Kim, Y.-H.; Kwon, S.-K.; Kim, B. J. Efficient, Thermally Stable, and Mechanically Robust All-Polymer Solar Cells Consisting of the Same Benzodithiophene Unit-Based Polymer Acceptor and Donor with High Molecular Compatibility. *Adv. Energy Mater.* **2021**, *11*, 2003367.
(70) Zhou, L.; Xia, X.; Meng, L.; Zhang, J.; Lu, X.; Li, Y. Introducing Electron-Withdrawing Linking Units and Thiophene π-Bridges into Polymerized Small Molecule Acceptors for High-Efficiency All-Polymer Solar Cells. *Chem. Mater.* **2021**, *33*, 8212−8222.
(71) Zhou, L.; Meng, L.; Zhang, J.; Qin, S.; Guo, J.; Li, X.; Xia, X.; Lu, X.; Li, Y. Effect of Isomerization of Linking Units on the Photovoltaic Performance of PSMA-Type Polymer Acceptors in All-Polymer Solar Cells. *Macromolecules* **2022**, *55*, 4420−4428.
(72) Wang, Y.; Wang, N.; Yang, Q.; Zhang, J.; Liu, J.; Wang, L. A Polymer Acceptor Containing the B←N Unit for All-Polymer Solar Cells with 14% Efficiency. *J. Mater. Chem. A* **2021**, *9*, 21071−21077.
(73) Sun, H.; Yu, H.; Shi, Y.; Yu, J.; Peng, Z.; Zhang, X.; Liu, B.; Wang, J.; Singh, R.; Lee, J.; Li, Y.; Wei, Z.; Liao, Q.; Kan, Z.; Ye, L.; Yan, H.; Gao, F.; Guo, X. A Narrow-Bandgap n-Type Polymer with an Acceptor−Acceptor Backbone Enabling Efficient All-Polymer Solar Cells. *Adv. Mater.* **2020**, *32*, 2004183.
(74) Sun, H.; Liu, B.; Ma, Y.; Lee, J.-W.; Yang, J.; Wang, J.; Li, Y.; Li, B.; Feng, K.; Shi, Y.; Zhang, B.; Han, D.; Meng, H.; Niu, L.; Kim, B. J.; Zheng, Q.; Guo, X. Regioregular Narrow-Bandgap n-Type Polymers with High Electron Mobility Enabling Highly Efficient All-Polymer Solar Cells. *Adv. Mater.* **2021**, *33*, 2102635.

(75) Chen, D.; Liu, S.; Hu, X.; Wu, F.; Liu, J.; Zhou, K.; Ye, L.; Chen, L.; Chen, Y. Printable and Stable All-Polymer Solar Cells Based on Non-Conjugated Polymer Acceptors with Excellent Mechanical Robustness. *Sci. China Chem.* **2022**, *65*, 182−189.
(76) Fan, Q.; Ma, R.; Liu, T.; Yu, J.; Xiao, Y.; Su, W.; Cai, G.; Li, Y.; Peng, W.; Guo, T.; Luo, Z.; Sun, H.; Hou, L.; Zhu, W.; Lu, X.; Gao, F.; Moons, E.; Yu, D.; Yan, H.; Wang, E. High-Performance All-Polymer Solar Cells Enabled by a Novel Low bandgap Non-Fully Conjugated Polymer Acceptor. *Sci. China Chem.* **2021**, *64*, 1380−1388.
(77) Genene, Z.; Lee, J.-W.; Lee, S.-W.; Chen, Q.; Tan, Z.; Abdulahi, B. A.; Yu, D.; Kim, T.-S.; Kim, B. J.; Wang, E. Polymer Acceptors with Flexible Spacers Afford Efficient and Mechanically Robust All-Polymer Solar Cells. *Adv. Mater.* **2022**, *34*, 2107361.
(78) Liu, J.; Liu, J.; Deng, J.; Huang, B.; Oh, J.; Zhao, L.; Liu, L.; Yang, C.; Chen, D.; Wu, F.; Chen, L. Non-Conjugated Terpolymer Acceptors for Highly Efficient and Stable Lager-Area All-Polymer Solar Cells. *J. Energy Chem.* **2022**, *71*, 631−638.
(79) Seo, S.; Sun, C.; Lee, J.-W.; Lee, S.; Lee, D.; Wang, C.; Phan, T. N.-L.; Kim, G.-U; Cho, S.; Kim, Y.-H.; Kim, B. J. Importance of High-Electron Mobility in Polymer Acceptors for Efficient All-Polymer Solar Cells: Combined Engineering of Backbone Building Unit and Regioregularity. *Adv. Funct. Mater.* **2022**, *32*, 2108508.
(80) Su, N.; Ma, R.; Li, G.; Liu, T.; Feng, L.-W.; Lin, C.; Chen, J.; Song, J.; Xiao, Y.; Qu, J.; Lu, X.; Sangwan, V. K.; Hersam, M. C.; Yan, H.; Facchetti, A.; Marks, T. J. High-Efficiency All-Polymer Solar Cells with Poly-Small-Molecule Acceptors Having π-Extended Units with Broad Near-IR Absorption. *ACS Energy Lett.* **2021**, *6*, 728−738.
(81) Liao, C.; Gong, Y.; Xu, X.; Yu, L.; Li, R.; Peng, Q. Cost-Efficiency Balanced Polymer Acceptors Based on Lowly Fused Dithienopyrrolo[3,2b]Benzothiadiazole for 16.04% Efficiency All-Polymer Solar Cells. *Chem. Eng. J.* **2022**, *435*, 134862.
(82) Sun, C.; Lee, J.-W.; Seo, S.; Lee, S.; Wang, C.; Li, H.; Tan, Z.; Kwon, S.-K.; Kim, B. J.; Kim, Y.-H. Synergistic Engineering of Side Chains and Backbone Regioregularity of Polymer Acceptors for High-Performance All-Polymer Solar Cells with 15.1% Efficiency. *Adv. Energy Mater.* **2022**, *12*, 2103239.
(83) Zhou, D.; Liao, C.; Peng, S.; Xu, X.; Guo, Y.; Xia, J.; Meng, H.; Yu, L.; Li, R.; Peng, Q. Binary Blend All-Polymer Solar Cells with a Record Efficiency of 17.41% Enabled by Programmed Fluorination Both on Donor and Acceptor Blocks. *Adv. Sci.* **2022**, *9*, 2202022.
(84) Zhang, Z. G.; Li, Y. Polymerized Small-Molecule Acceptors for High-Performance All-Polymer Solar Cells. *Angew. Chem., Int. Ed.* **2021**, *60*, 4422−4433.
(85) Yu, X.; Lin, H.; Li, M.; Ma, B.; Zhang, R.; Du, X.; Zheng, C.; Yang, G.; Tao, S. Ternary Organic Solar Cells with Enhanced Charge Transfer and Stability Combining the Advantages of Polymer Acceptors and Fullerene Acceptors. *Org. Electron.* **2022**, *104*, 106471.
(86) Sun, Y.; Ma, R.; Kan, Y.; Liu, T.; Zhou, K.; Liu, P.; Fang, J.; Chen, Y.; Ye, L.; Ma, C.; Yan, H.; Gao, K. Simultaneously Enhanced Efficiency and Mechanical Durability in Ternary Solar Cells Enabled by Low-cost Incompletely Separated Fullerenes. *Macromol. Rapid Commun.* **2022**, 2200139.
(87) Li, Z.; Peng, F.; Ying, L.; Quan, H.; Li, J.; Wang, X.; Wu, H.; Huang, F.; Cao, Y. Fine-Tuning Miscibility of Donor/Acceptor through Solid Additives Enables All-Polymer Solar Cells with 15.6% Efficiency. *Sol. RRL* **2021**, *5*, 2100549.
(88) Liu, T.; Yang, T.; Ma, R.; Zhan, L.; Luo, Z.; Zhang, G.; Li, Y.; Gao, K.; Xiao, Y.; Yu, J.; Zou, X.; Sun, H.; Zhang, M.; Dela Pena, T. A.; Xing, Z.; Liu, H.; Li, X.; Li, G.; Huang, J.; Duan, C.; Wong, K. S.; Lu, X.; Guo, X.; Gao, F.; Chen, H.; Huang, F.; Li, Y.; Li, Y.; Cao, Y.; Tang, B.; Yan, H. 16% Efficiency All-Polymer Organic Solar Cells Enabled by a Finely Tuned Morphology *via* the Design of Ternary Blend. *Joule* **2021**, *5*, 914−930.
(89) Ma, R.; Yu, J.; Liu, T.; Zhang, G.; Xiao, Y.; Luo, Z.; Chai, G.; Chen, Y.; Fan, Q.; Su, W.; Li, G.; Wang, E.; Lu, X.; Gao, F.; Yan, H.; Tang, B. All-Polymer Solar Cells with Over 16% Efficiency and Enhanced Stability Enabled by Compatible Solvent and Polymer Additives. *Aggregate* **2022**, *3*, e58.
(90) Hu, K.; Du, J.; Zhu, C.; Lai, W.; Li, J.; Xin, J.; Ma, W.; Zhang, Z.; Zhang, J.; Meng, L.; Li, Y. Chlorinated Polymerized Small Molecule Acceptor Enabling Ternary All Polymer Solar Cells with Over 16.6% Efficiency. *Sci. China Chem.* **2022**, *65*, 954−963.
(91) Chen, D.; Liu, S.; Huang, B.; Oh, J.; Wu, F.; Liu, J.; Yang, C.; Chen, L.; Chen, Y. Rational Regulation of the Molecular Aggregation Enables A Facile Blade-Coating Process of Large-area All-Polymer Solar Cells with Record Efficiency. *Small* **2022**, *18*, 2200734.
(92) Sun, R.; Wang, W.; Yu, H.; Chen, Z.; Xia, X.; Shen, H.; Guo, J.; Shi, M.; Zheng, Y.; Wu, Y.; Yang, W.; Wang, T.; Wu, Q.; Yang, Y. M.; Lu, X.; Xia, J.; Brabec, C. J.; Yan, H.; Li, Y.; Min, J. Achieving Over 17% Efficiency of Ternary All-Polymer Solar Cells with Two Well-Compatible Polymer Acceptors. *Joule* **2021**, *5*, 1548−1565.
(93) Hu, K.; Du, J.; Sun, C.; Zhu, C.; Zhang, J.; Yao, J.; Zhang, Z.; Wan, Y.; Zhang, Z.; Meng, L.; Li, Y. Ternary All-Polymer Solar Cells with Two Synergetic Donors Enable Efficiency over 14.5%. *Energy Fuels* **2021**, *35*, 19045−19054.
(94) Zhang, W.; Sun, C.; Angunawela, I.; Meng, L.; Qin, S.; Zhou, L.; Li, S.; Zhuo, H.; Yang, G.; Zhang, Z.-G.; Ade, H.; Li, Y. 16.52% Efficiency All-Polymer Solar Cells with High Tolerance of the Photoactive Layer Thickness. *Adv. Mater.* **2022**, *34*, 2108749.
(95) Li, S.; Yuan, X.; Zhang, Q.; Li, B.; Li, Y.; Sun, J.; Feng, Y.; Zhang, X.; Wu, Z.; Wei, H.; Wang, M.; Hu, Y.; Zhang, Y.; Woo, H. Y.; Yuan, J.; Ma, W. Narrow-Bandgap Single-Component Polymer Solar Cells with Approaching 9% Efficiency. *Adv. Mater.* **2021**, *33*, 2101295.
(96) Wu, Y.; Guo, J.; Wang, W.; Chen, Z.; Chen, Z.; Sun, R.; Wu, Q.; Wang, T.; Hao, X.; Zhu, H.; Min, J. A Conjugated Donor-Acceptor Block Copolymer Enables Over 11% Efficiency for Single-Component Polymer Solar Cells. *Joule* **2021**, *5*, 1800−1815.
(97) Guo, J.; Wu, Y.; Wang, W.; Wang, T.; Min, J. Achieving 12.6% Efficiency in Single-Component Organic Solar Cells Processed from Nonhalogenated Solvents. *Sol. RRL* **2022**, *6*, 2101024.
(98) Zhao, T.; Cao, C.; Wang, H.; Shen, X.; Lai, H.; Zhu, Y.; Chen, H.; Han, L.; Rehman, T.; He, F. Highly Efficient All-Polymer Solar Cells From A Dithieno [3, 2-F: 2′, 3′-H] Quinoxaline-Based Wide Band Gap Donor. *Macromolecules* **2021**, *54*, 11468−11477.
(99) Shi, Y.; Ma, R.; Wang, X.; Liu, T.; Li, Y.; Fu, S.; Yang, K.; Wang, Y.; Yu, C.; Jiao, L.; Wei, X.; Fang, J.; Xue, D.; Yan, H. Influence of Fluorine Substitution on the Photovoltaic Performance of Wide Band Gap Polymer Donors for Polymer Solar Cells. *ACS Appl. Mater. Interfaces* **2022**, *14*, 5740−5749.
(100) Wu, X.; Hao, X.; Deng, P.; Chen, H. A Y6-Based Polymerized Small-Molecule Acceptor with Non-Conjugated Alkyl Linkages for Efficient All-Polymer Solar Cells. *Dyes Pigm.* **2021**, *196*, 109824.
(101) Jia, T.; Zhang, J.; Zhang, K.; Tang, H.; Dong, S.; Tan, C. H.; Wang, X.; Huang, F. All-Polymer Solar Cells with Efficiency Approaching 16% Enabled Using a Dithieno[3′,2′:3,4;2″,3″:5,6]-benzo[1,2-c][1,2,5]thiadiazole (Fdtbt)-Based Polymer Donor. *J. Mater. Chem. A* **2021**, *9*, 8975−8983.
(102) Li, Y.; Deng, D.; Sun, R.; Wu, S.; Zhang, L.; Zhang, Z.; Zhang, J.; Min, J.; Zhao, G.; Wei, Z. Efficient Charge Generation and Low Open Circuit Voltage Loss Enable a PCE of 10.3% in Small Molecule Donor and Polymer Acceptor Organic Solar Cells. *J. Mater. Chem. C* **2022**, *10*, 2639.
(103) Liu, W.; Xu, S.; Lai, H.; Liu, W.; He, F.; Zhu, X. Near-Infrared All-Fused-Ring Nonfullerene Acceptors Achieving an Optimal Efficiency-Cost-Stability Balance in Organic Solar Cells. *CCS Chem.* **2022**, 1−15.
(104) Wu, B.; Zhang, Y.; Tian, S.; Oh, J.; Yang, M.; Pan, L.; Yin, B.; Yang, C.; Duan, C.; Huang, F.; Cao, Y. Non-Fused Polymerized Small Molecular Acceptors for Efficient All-Polymer Solar Cells. *Sol. RRL* **2022**, *6*, 2101034.
(105) Zhu, J.; Shao, Z.; Wang, J.; Sun, D.; Zhu, M.; Song, X.; Tan, H.; Zhu, W. Non-Fused-Ring Asymmetrical Electron Acceptors Assembled by Multi-Functional Alkoxy Indenothiophene unit to Construct Efficient Organic Solar Cells. *Chem. Eng. J.* **2022**, *444*, 136509.
(106) Song, X.; Xu, Y.; Tao, X.; Gao, X.; Wu, Y.; Yu, R.; He, Y.; Tao, Y. BODIPY Cored A− D− A′− D− A Type Nonfused-Ring Electron

Acceptor for Efficient Polymer Solar Cells. *Macromol. Rapid Commun.* **2022**, 2100828.
(107) Ji, J.; Zhu, L.; Xiong, X.; Liu, F.; Liang, Z. Developing Y-Branched Polymer Acceptor with 3D Architecture to Reconcile Between Crystallinity and Miscibility Yielding> 15% Efficient All-Polymer Solar Cells. *Adv. Sci.* **2022**, *9*, 2200864.
(108) Zhang, L.; Zhang, Z.; Deng, D.; Zhou, H.; Zhang, J.; Wei, Z. N-π-N" Type Oligomeric Acceptor Achieves an OPV Efficiency of 18.19% with Low Energy Loss and Excellent Stability. *Adv. Sci.* **2022**, *9*, 2202513.
(109) Liu, W.; Yuan, J.; Zhu, C.; Wei, Q.; Liang, S.; Zhang, H.; Zheng, G.; Hu, Y.; Meng, L.; Gao, F.; Li, Y.; Zou, Y. A-π-A Structured Non-Fullerene Acceptors for Stable Organic Solar Cells with Efficiency Over 17%. *Sci. China Chem.* **2022**, *65*, 1374−1382.
(110) Cao, C.; Wang, H.; Qiu, D.; Zhao, T.; Zhu, Y.; Lai, X.; Pu, M.; Li, Y.; Li, H.; Chen, H.; He, F. Quasiplanar Heterojunction All-Polymer Solar Cells: A Dual Approach to Stability. *Adv. Funct. Mater.* **2022**, *32*, 2201828.
(111) Xu, X.; Yu, L.; Meng, H.; Dai, L.; Yan, H.; Li, R.; Peng, Q. Polymer Solar Cells with 18.74% Efficiency: From Bulk Heterojunction to Interdigitated Bulk Heterojunction. *Adv. Funct. Mater.* **2022**, *32*, 2108797.
(112) Li, B.; Zhang, X.; Wu, Z.; Yang, J.; Liu, B.; Liao, Q.; Wang, J.; Feng, K.; Chen, R.; Woo, H. Y.; Ye, F.; Niu, L.; Guo, X.; Sun, H. Over 16% Efficiency All-Polymer Solar Cells by Sequential Deposition. *Sci. China Chem.* **2022**, *65*, 1157−1163.
(113) Cui, F. Z.; Chen, Z. H.; Qiao, J. W.; Wang, T.; Lu, G. H.; Yin, H.; Hao, X. T. Ternary-Assisted Sequential Solution Deposition Enables Efficient All-Polymer Solar Cells with Tailored Vertical-Phase Distribution. *Adv. Funct. Mater.* **2022**, *32*, 2200478.
(114) Zhang, Y.; Wu, B.; He, Y.; Deng, W.; Li, J.; Li, J.; Qiao, N.; Xing, Y.; Yuan, X.; Li, N.; Brabec, C. J.; Wu, H.; Lu, G.; Duan, C.; Huang, F.; Cao, Y. Layer-by-layer processed binary all-polymer solar cells with efficiency over 16% enabled by finely optimized morphology. *Nano Energy* **2022**, *93*, 106858.

https://doi.org/10.1021/acsenergylett.2c01541
ACS Energy Lett. 2022, 7, 3835−3854